The Application of BEASY Software to Simulate Cathodic Protection of

Pipelines and Storage Tanks

by

Mohammed Al-Otaibi

B.Sc., King Abdul-Aziz University, 2004

A THESIS SUBMITTED IN PARTIAL FULFILLMENT OF
THE REQUIRMENTS FOR THE DEGREE OF

MASTER OF APPLIED SCIENCE

in

THE FACULTY OF GRADUATE STUDIES

(Materials Engineering)

THE UNIVERSITY OF BRITISH COLUMBIA
(Vancouver)

November 2010

Abstract

Cathodic protection is used in the mitigation and control of corrosion in the petrochemical and oil industries. To test and predict the level of metal protection effectively, various simulation and testing methods have been developed to provide timely and cost effective solutions. The purpose of this study is to match the data generated by the BEASY software with the experimental output data so that the BEASY software can be applied in the field with a high degree of confidence.

In the first experiment, Boundary Element Analysis software BEASY has been utilized to test sacrificial cathodic protection. Pure zinc was used to protect a mild steel plate in an aqueous solution. Next, high silicon cast iron or copper was connected to a mild steel plate both of which were protected by a zinc anode. In the final application experiment of sacrificial cathodic protection, the BEASY software was used to investigate the failure of the magnesium anode in an alkaline solution. The possibility to use aluminum alloy as an anode instead of magnesium was also studied.

As for the impress current cathodic protection, the BEASY software was used to simulate a small section of carbon steel pipe segment which was protected in sand soil by a high silicon cast iron anode. Additionally, a real impress current cathodic protection system designed for 12 pipes protected with six anodes has been simulated.

The results of from the simulation and the experimental data generated by the performed experiments have confirmed the soundness and applicability of the BEM BEASY software in the industrial applications.

Table of Contents

List of tables

List of figures

List of symbols

A	area (m^2).
A	matrix includes unknowns H and G.
a	molecular mass (g mol^{-1})
B	matrix includes known variables.
b	Tafel slope (mV)
c	concentration (mol m^3)
d	diameter (cm)
D	diffusion coefficient ($m^2\ s^{-1}$)
$\mathbf{e}$	vector of error in iteration process
E	electrochemical potential (mV)
Ea	electrochemical potential on the anode surface (mV)
Ec	electrochemical potential on the cathode surface (mV)
$E*$	fundamental solution of the potential (mV)
E_j^m	potential in m-th iteration associated with node j (mV)
E_j^{m+1}	potential in m+1-th iteration associated with node j (mV)
ΔE_j^m	increment of potential in m-th iteration associated with node j (mV)
F	Faraday's constant = 96485 A s mol^{-1}
H, G	square matrices of influence coefficient of system geometry.
I	current density (A cm^{-2})
Ia	current density on the anode surface (A cm^{-2})
Ic	current density on the cathode surface (A cm^{-2})
$I*$	fundamental solution of the current density (A cm^{-2})
I_{a1}	current density generated by iron oxidation (A cm^{-2})
I_{c1}	current density generated by oxygen reduction (A cm^{-2})
I_{c2}	current density generated by hydrogen evolution (A cm^{-2})
I_j^m	current density in m-th iteration associated with node j (A cm^{-2})
I_j^{m+1}	current density in m+1-th iteration associated with node j (A cm^{-2})

ΔI_j^m increment of current density in m-th iteration associated with node j

$(A\ cm^{-2})$

J   Jacobian of the system of equations

k conductivity $(S\ m^{-1})$

l length (cm)

N   number of nodes on the boundary

n   number of electrons required for the reactions

R resistance (Ω)

r_c corrosion rate $(g\ m^{-2}\ day^{-1})$

r   distance from the source point (cm)

R_P pipe electrical resistance per meter $(\Omega\ m^{-1})$

t pipes wall thickness (cm)

u   mechanical mobility $(m^2\ N^{-1}\ s^{-1})$

X matrix includes unknowns I and E

x_i position or length (cm)

z   charge (coulomb)

Greek Symbols

α , β constants characterizing polarization curves (mV)

Γ boundary surrounding the electrolyte

Γa anode surface boundary

Γc cathode surface boundary

δ_{ij} Kronecker delta,

ε allowable error in iteration

ξ source point (position on the geometry)

η over potential (mV)

ρ resistivity (Ω-cm)

Ω homogeneous electrolyte

Acknowledgments

First of all, I would like to thank my supervisor, Dr. Akram Alfantazi for his direction and guidelines during the course of my thesis development. Without his support and encouragement, I would not have been able to finish the research work. I was always happy to know that Dr. Alfantazi was there for me in case I did not move forward with my study fast enough. His intellect and insights have inspired me in the right direction. I also thank Dr. Edouard Asselin for his valuable discussions and directions during the research work.

Throughout the research and writing process, there were many occasions that I was not able to progress. Whenever that happened, my wife was also there for me. I regret not spending more time with my lovely two kids, Yasser and Jana.

I truly enjoy working at Saudi Basic Industries Corporation (SABIC) that provided funding for my study at UBC. Without their financial assistance, it would be challenging to study abroad. I thank Mr. Ali Al-Hazemi for his support. I look forward to going back and working for SABIC.

Chapter 1

Introduction

Cathodic Protection (CP) is a technique to control the corrosion of a metal surface by making it work as a cathode of an electrochemical cell. There are two types of the CP: Sacrificial Cathodic Protection that occurs when a metal is coupled with a more reactive (anodic) metal and Impressed Current Cathodic Protection which involves the application of an external direct current (DC) through long-lasting anodes. However, to justify the use of a CP system, there ought to be some means of testing it before in-field application.

The simulation of cathodic protection provides a prediction about the system performance before installation. This technique reduces the dependency on the individual experience of a CP Engineer and on the simple formulas that are used in designing the CP system. Moreover, a cathodic protection simulation gives useful parameters: e.g. degree of protection, corrosion rate, DC power supply rate etc. to improve integrity of the CP system. Historically, numerical methods have been demonstrated to be powerful tools in the analysis of corrosion problems since the early 1980's. They started by the Finite Difference Method (FDM); then Finite Element Method (FEM) was used; finally Boundary Element Method (BEM) makes the simulation simpler. The BEM has a number of advantages over the other two methods (FDM and FEM). These advantages include [Santana-Diaz, 2006]:

- The meshes are only on the surface, so mesh generation can be used with confidence, and a CP model can be constructed quickly and inexpensively.

- The BEM gives the solutions on the boundary and at the specific internal points if required. Since, for CP analysis, the solution is only required on the surfaces. It analyzes the results better than the FEM which automatically gives results for all nodes (internal or boundary).

- BEM methods are very effective and accurate for modeling infinite domains as is the case for long pipelines.

There are practical examples that validate the simulation of cathodic protection. A number of metallic structures have been modeled by the BEM: namely, ships, off-shore oil structures, Floating Production Storage and Offloading (FPSO), pipelines, tanks and well casing. Furthermore, there are issues that ought to be considered in the simulation of cathodic protection systems. Potentially, the most important issues are the cathodic protection interference, optimum location of the anodes and reference electrode and the influence of coatings.

1.1 Scope and objective

The objective of this research is to confirm the data generated by the BEASY software with our own experimental results so that the BEASY end result data can be applied in the field with confidence. Three experiments are conducted to ascertain the validity of the software output.

In the first experiment, Boundary Element Analysis software BEASY has been chosen as it is an advanced program for modeling the cathodic protection to test sacrificial cathodic protection. In this experiment, pure zinc was used to protect mild steel plate in aqueous solution. Then another material (high silicon cast iron and copper) was connected to a mild

steel plate. In the final application experiment, the BEASY software was used to investigate the failure of magnesium anodes in alkaline solution. The possibility to use aluminum alloy as an anode instead of magnesium was studied.

Next, the BEASY software was used to simulate a small section of carbon steel pipe segment, buried in sand soil which was protected by the high silicon cast iron anode. Additionally a real impress current cathodic protection system designed for 12 pipes protected with six anodes has been simulated.

Chapter 2

Literature review

2.1 Cathodic protection

2.1.1 Introduction

Cathodic Protection (CP) is a technique to control the corrosion of a metal surface by making it work as a cathode of an electrochemical cell. This is achieved by the polarization of all noble potential areas (cathodes) to the most active potential on the metal surface. Cathodic protection is realized by making the structure a cathode of a direct current circuit.
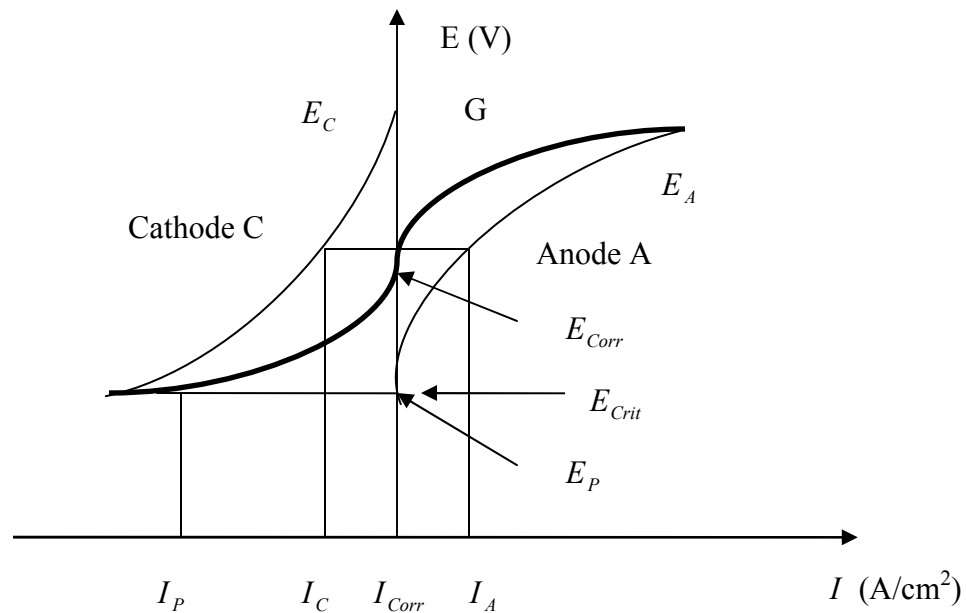
Fig. 2.1 Polarization curve for anodic and cathodic reaction [Wrobel, 2004].

CP is based upon bringing the galvanic potential of the metal to be protected to a level where anodic reactions are impossible for the given circumstances. The relationship between the potential and current density is generally described by a non-linear curve, known as

polarization curve. Fig.2.1 by Wrobel schematically depicts the polarization curve for both anodic and cathodic reaction. Curve A represents the relation between the electrochemical potential E and the current density I of the oxidation reaction of the metals in the given electrolyte, with related equilibrium potential E_A. Curve C represents a similar relation for the reduction equation, with related equilibrium potential E_c. The global curve G is the sum of the elementary reactions (anodic and cathodic) arising on the metals. The corrosion potential E_{corr} is related to the natural corrosion of the metal at given current density I_{corr}. This potential is reached when all anodic and cathodic zones are short-circuited. Fig.2.1 also shows that if the potential is lower than E_{crit}, for example E_p, the anodic reaction is stopped and the metal acts completely as a cathode under a protective current density I_p. [Wrobel, 2004] [Amaya, 2003].

Two Types of the Cathodic Protection (CP)

2.1.2 Sacrificial Cathodic Protection

Sacrificial Cathodic Protection occurs when a metal is coupled to a more reactive (anodic) metal. This connection is referred to as a galvanic couple. In order to effectively transfer corrosion from the metal structure, the anode material must have a large enough natural voltage difference to produce an electrical current flow. Effective application of cathodic protection can provide complete protection to any exposed areas for the life of the structure. Fig.2.2 illustrates a simplified polarization diagram for the galvanic couple between a sacrificial anode $E_{corr(a)}$ and the cathodically protected structure of $E_{corr(C)}$. The two are polarized to the same potential, Esc, with the galvanic current, $I_{G(sc)}$, following in the couple. At Esc the corrosion rate of the structure has been reduced from I_{corr} to $I_{corr(sc)}$. R is the

solution resistance between a sacrificial anode and cathode structure. With a resistance R, a potential, $I_{G(R)} R$ separate anode and cathode. The corrosion current density under potential decreases from $I_{corr(sc)}$ to $I_{corr(R)}$ by the presence of R, and the couple current density is reduced to $I_{G(R)}$.
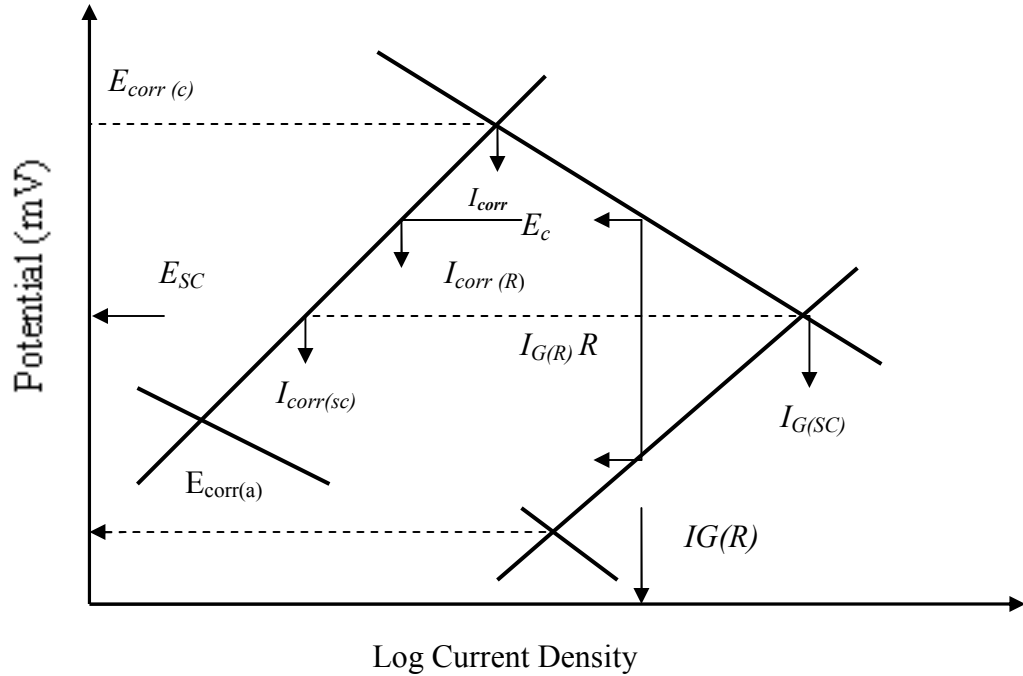
Fig.2.2 Schematic polarization diagram for a sacrificial cathodic protection [Jones, 1996].

Sacrificial Cathodic Protection systems are used where:

- The required current for protection is relatively small.

- There are constraints on the use of impress current

- Spot requirements

The most commonly used sacrificial or galvanic anodes materials are:

a) Zinc

Zinc has been used for protection in seawater since 1824. In the beginning, zinc material that was available from the hot-dip galvanizing industry was used but was less suitable because it became passive to zinc carbonate $ZnCO_3$. Passivation does not occur with high-purity zinc. Super high grade zinc is the anode material with the least problems and consists of 99.995% Zn and less than 0.0014% Fe without further additions. Zinc anodes for use in salt-rich media do not need additional activating elements. In cathodic protection, zinc is used in low soil resistivity or saltwater. [Baeckmann, 1997].

b) Aluminum

Pure aluminum cannot be used as an anode material on account of its easy passive ability. For galvanic anode, aluminum alloys are employed that contain activating alloying elements that hinder or prevent the formation of surface films. These are usually up to 8% Zn and/or 5% Mg. In addition, metals such as Cd, Ga, In, Hg and Ti are added to maintain the long-term activity of the anode. The aluminum anode is used in the area of offshore structures where pure seawater flows with a high velocity. [Baeckmann, 1997].

c) Magnesium

Magnesium anode is considerably less passive than zinc and aluminum alloy and has the highest driving voltage. On account of these properties, magnesium is particularly suitable for galvanic anode. Magnesium, however, is prone to self corrosion of considerable extent, which increases with increasing salt content of medium. Magnesium anodes are used in the case of higher specific resistivity of the electrolyte and higher protection current densities. [Baeckmann, 1997].

2.1.3 Impress current cathodic protection (ICCP)

Impressed current cathodic protection involves the application of an external DC current through long-lasting anodes. A typical source of power for an impressed current system is AC power converted to DC by a rectifier.

In order to be effective, impressed current anodes must be designed for long life at high current output. This requires selection of materials with very low corrosion (consumption) rates. The typical expectation of impressed current anode life is over twenty years. Anodes are normally installed in grouped configurations in the electrolyte. These groupings (both horizontal and vertical) in an underground application are called groundbeds. The groundbeds are connected to the power by a positive cable. A negative cable connects the power source to the structure.

Fig.2.3 shows an impress current cathodic protection diagram of steel in natural aerated water or seawater. Diffusion of dissolved oxygen to the corroding surface controls corrosion. Because the applied current and corrosion rate are limited by I_L, the I_{app} is the amount of applied current density by impress current to protect the steel.
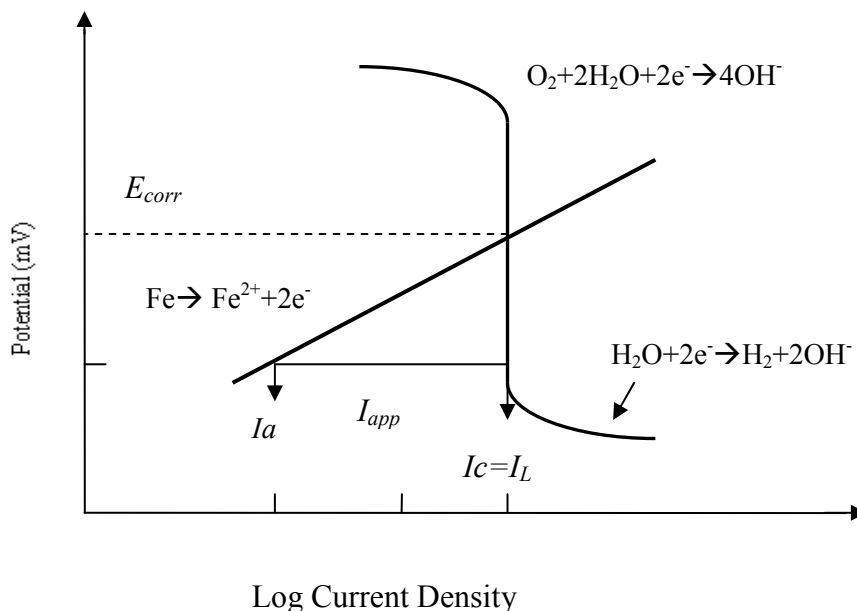
Fig. 2.3 Cathodic protection by impress current density, I_{app} for steel in natural aerated water.

Advantage of ICCP:

- Can be designed for a wide range of voltage and current output.

- High ampere/year output available from single anode installation.

- Large area can be protected.

- Variable voltage and current output.

- Applicable for high resistivity soil.

Disadvantages of ICCP:

- The requirement for an outside power source

- Higher maintenance requirements.

- A significantly higher monitoring and maintenance effort is required in comparison to sacrificial anode systems.

The outside power might come from sources such as commercial AC converted to DC through a rectifier, thermoelectric generator, or solar panels.

The most commonly used impress current anodes are:

a) High silicon cast iron.

b) Graphite.

c) Platinum.

d) Mixed metal oxide

2.2 Numerical simulation of cathodic protection

2.2.1 Introduction

The majority of design for the CP systems in the past has relied upon simple formulas, skills and experience of the CP engineer. Evaluations of CP systems take place after

commissioning. Moreover, after commissioning, the adjustment of a CP system will lead to re-installation costs, production downtime and disrupted schedules. Therefore, the modeling of a CP system will help forecast the following:

- The degree of potential protection which is provided by a CP system.

- The corrosion rate.

- The anode consumption rate.

- The total current demand and how it changes with time.

- The life expectancy of an anode.

- The optimum location of anodes.

- The optimum location of reference electrodes.

- The DC power supply capacity requirement.

Numerical methods have been powerful tools in the analysis of corrosion problems since the early 1980's. Numerical methods applied to corrosion problems have included the Finite Difference Method (FDM). Finite Element Method (FEM) was also applied in this field by Montoya [Montoya, 2005] together with Boundary Element Method (BEM). As corrosion and cathodic protection are surface phenomena, the BEM method has distinct advantages over the other two methods. One of the main advantages of BEM is that descritizations are restricted only to the boundaries, making data generation much easier. The BEM is also ideally suited for analysis of external problems where domains extend to infinity. Therefore, the above advantages make the BEM superior than the FDM and the FEM in the simulation of a cathodic protection system.

2.2.2 Boundary Element simulation software

A number of software based on Boundary Element Method are available to simulate corrosion and cathodic protection: e.g. PROCOR, SEACORR, ELSYCA, BEASY, OKAPPI and PROCAT. Some of these software are designed for a specific application. Boundary Element Analysis System (BEASY) has been chosen based on wide acceptance by the literature. Moreover, the BEASY software provides required options needed to simulate many structures that are protected by cathodic protection systems. While non-BEASY software has special versions for each structure such as tanks, pipes, or ships.

2.2.3 Mathematical aspect of the Boundary Element Method

The mathematical model of corrosion and cathodic protection based on Boundary Element Method has been applied to the field since 1980's. The background and the formulas were provided by many pervious researches that come across the modeling of cathodic protection [Chuang, 1987] [Yan, 1992] [Santiago, 1997] [Santiago, 1999] [Ramana, 1999] [Colominas, 1999] [Sun, 2000 A] [Sun, 2000 B] [Amaya, 2003] [Miltiadous, 2004] [Wrobel, 2004] [Jia, 2004] [Lacerda, 2007].

To quantify the protection potential and current density discussed in Fig. 2.1

The current density can be defined as [Wrobel, 2004]

$$Ij = -F\sum_{i=1}^{N} z_i D_i \frac{\partial c_i}{\partial x_i} - F^2 \sum_{i=1}^{N} z_i^2 c_i u_i \frac{\partial E}{\partial x_i} \qquad (1)$$

Where Ij is the component of the current density vector; F is Faraday's constant; z_i, c_i, u_i and D_i are the charge, concentration, mechanical mobility and diffusion coefficient, respectively. For species i, N is the number of species and E is the electrochemical potential. Defining the conductivity of the electrolyte in the form [Wrobel, 2004]

11

$$k = F^2 \sum_{i=1}^{N} z_i^{\,2} c_i u_i \qquad\qquad (2)$$

The above equation reduces to:

$$Ij = -F \sum_{i=1}^{N} z_i D_i \frac{\partial c_i}{\partial x_i} - k \frac{\partial E}{\partial x_i} \qquad\qquad (3)$$

The first term of the above equation represents the portion of current density sustained by concentration gradients, and this term can be neglected in large scale simulations, because concentration gradients exist only in the diffusion layer which is very thin compared to the size of simulation domain. Therefore, the current density in the electrolyte is then given by:

$$Ij = -k \frac{\partial E}{\partial x_i} \qquad \text{Current density in electrolyte} \qquad (4)$$

Conservation of charge gives

$$\frac{\partial Ij}{\partial x_i} = \frac{\partial}{\partial x_i}\left(-k \frac{\partial E}{\partial x_i}\right) = 0 \qquad\qquad (5)$$

If the conductivity k is constant e.g. seawater so the above equation reduces to a Laplace equation for the electrochemical potential E [Adey, 1985]

$$k\nabla^2 E = 0 \qquad\qquad (6)$$

The above equation is the governing equation for the potential distribution in an electrolyte.
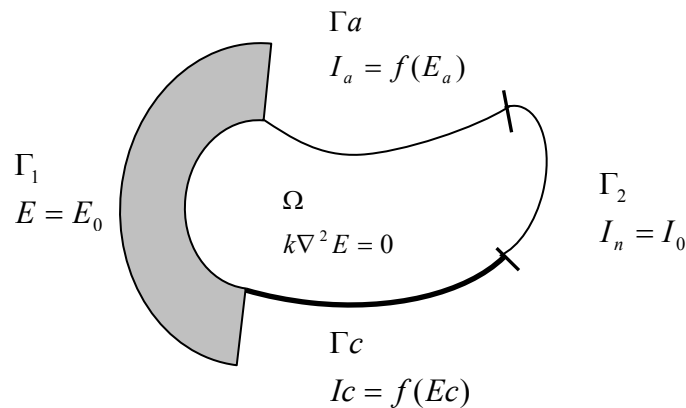
Fig. 2.4 Governing equation and boundary condition [Wrobel, 2004], [Santana-Diaz, 2005 B].

Consider that the CP system is designed within a homogeneous electrolyte Ω, surrounded by a boundary $\Gamma(\Gamma1 + \Gamma2 + \Gamma a + \Gamma c)$ as shown in the Fig. 2.4 where the electrochemical potential E or current density I are prescribed on $\Gamma1$ and $\Gamma2$ respectively, while Γa represent the anode surface and Γc is the cathode surface.

The boundary condition is

$$E = E_0 \qquad\qquad \text{On } \Gamma1$$

$$I_n = k\frac{\partial E}{\partial n} = I_0 \qquad\qquad \text{On } \Gamma2$$

$$Ia, Ea \text{ unknown} \qquad\qquad \text{on } \Gamma a$$

$$Ic, Ec \text{ unknown} \qquad\qquad \text{on } \Gamma c$$

We wish to solve (6) numerically as follows [Santana-Diaz, 2005 B]:

$$c(\xi)E(\xi) = \int_\Gamma E*(\xi,x)I_n d\Gamma(x) - \int_\Gamma I*(\xi,x)E(x)d\Gamma(x) \qquad\qquad (7)$$

Where $E*(\xi,x)$ and $I*(\xi,x)$ are the fundamental solution for the potential and current density respectively and the free term c (ξ) depends on the boundary geometry at the source point ξ.

$$E*(\xi,x) = \frac{1}{4\pi kr} \qquad\qquad\qquad (8)$$

$$I*(\xi,x) = k\frac{\partial E^*}{\partial n} \qquad\qquad\qquad (9)$$

Where r is the distance from the point x_i of application of the delta function to any point under consideration.

Since the boundary Γ is discretized into approximated number of boundary elements N [Santana-Diaz, 2005 B]

$$c_i E_i + \sum_{j=1}^{N} Ej \int_{\Gamma} I^* d\Gamma j = \sum_{j=1}^{N} Ij \int_{\Gamma} E^* d\Gamma j \qquad (10)$$

Where $\int_{\Gamma j}$ represents integration over element j. The terms $\hat{H} ij$ and Gij are obtained as

follows [Santana-Diaz, 2005 B]

$$\hat{H} ij = \int_{\Gamma} I^* d\Gamma j \qquad (11)$$

$$Gij = \int_{\Gamma} E^* d\Gamma j \qquad (12)$$

And

$$Hij = \hat{H} ij + ci\delta_{ij} \qquad (13)$$

Where δ_{ij} is the Kronecker delta, $\delta ij = \begin{cases} 1, if & i=j \\ 0, if & i \neq j \end{cases}$

The following algebraic system is obtained [Santana-Diaz, 2005 B]

$$\sum_{j=1}^{N} HijE = \sum_{j=1}^{N} GijI \qquad (14)$$

If equation 14 applied to all nodal points along the boundary, the following equation is

obtained:

HE = GI   (15)

Where **H** and **G** are square matrices of influence coefficient, **E** and **I** are vectors of nodal

values of potential and current density.

Some of the elements of the vector **E** and vector **I** are known while some are unknown. By

arranging all knowns on the right hand side and all unknowns on the left,

The following matrix equation is obtained [Adey, 1985]

AX=B   (16)

To partition the E and I vectors (matrices (15)) into those nodes which form the anode and those which form the cathodes as follows [Adey, 1985]

$$\begin{bmatrix} Haa & Hac \\ Hca & Hcc \end{bmatrix}\begin{bmatrix} Ea \\ Ec \end{bmatrix} = \begin{bmatrix} Gaa & Gac \\ Gca & Gcc \end{bmatrix}\begin{bmatrix} Ia \\ Ic \end{bmatrix} \tag{17}$$

"a" refers to anode surface and "c" refers to cathode surface

$$\begin{aligned} Ia &= f(Ea), \\ Ic &= f(Ec). \end{aligned} \tag{18}$$

Substituting equation (16) [Adey, 1985]:

$$\begin{bmatrix} Haa & Hac \\ Hca & Hcc \end{bmatrix}\begin{bmatrix} Ea \\ Ec \end{bmatrix} = \begin{bmatrix} Gaa & Gac \\ Gca & Gcc \end{bmatrix}\begin{bmatrix} fa(Ea) \\ fc(Ec) \end{bmatrix} \tag{19}$$

The resulting Eq. (19) is solved by iteration in Fig.2.5 to obtain the current density I and potential E at all nodes on the anode and cathode.

START

Calculate **G. H**

Specify E_0 on Anode

Make Ec on cathode
Ia on anode

Calculate I on cathode
from $I = f(E)$

$\mathrm{e} = GI - HE$

$|error| \langle \varepsilon$

No

$J\delta = -e$

$E_j^{m+1} = E_j^m + \Delta E_j^m$

$I_j^{m+1} = I_j^m + \Delta I_j^m$

Yes

E, I

END
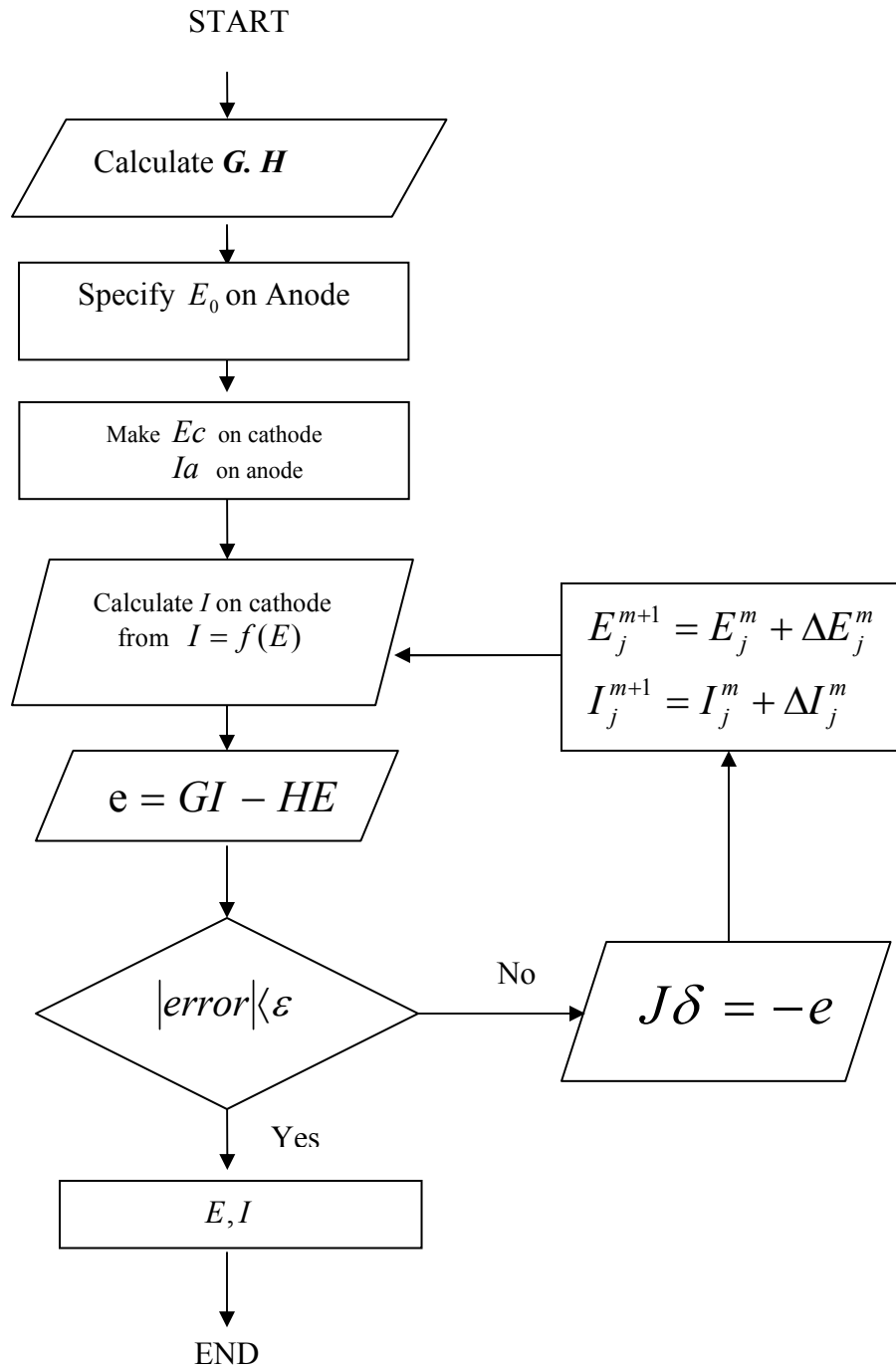
Fig. 2.5 Flow chart of the iteration algorithm in solving a cathodic protection problem using BEM. [Yan, 1992].

16

2.3 Simulation of different structures

2.3.1 Simulation of the offshore structure

2.3.1.1 Ships

The cathodic protection of ships was the first practice of simulation because the electrolyte is relatively uniform (Seawater) surrounding the ship body. There are two critical parts on the ship that need to be catholically protected:

Ship Hull

Ship hull is the largest part of the ship. It has to be coated and the cathodic protection is applied to protect the coating holidays on the surface. The anodes that protect the ship shall be mounted on each side of the hull. Zamani [Zamani, 1988] applied the Boundary Element Method to simulate the cathodic protection on prototype ship mathematically. He applied to a prototype operating in the eastern fleet of Canadian navy. The difference between the measured and the calculated potential result was 6% which is generally acceptable. Sun [Sun, 1996] has studied the optimal control of impress current which protects bare and painted surface of a ship. The model was solved numerically by using two anodes in each side of the ship's hull but the prediction potential was low. Then Sun increased the number of anodes to five to improve the potential distribution.
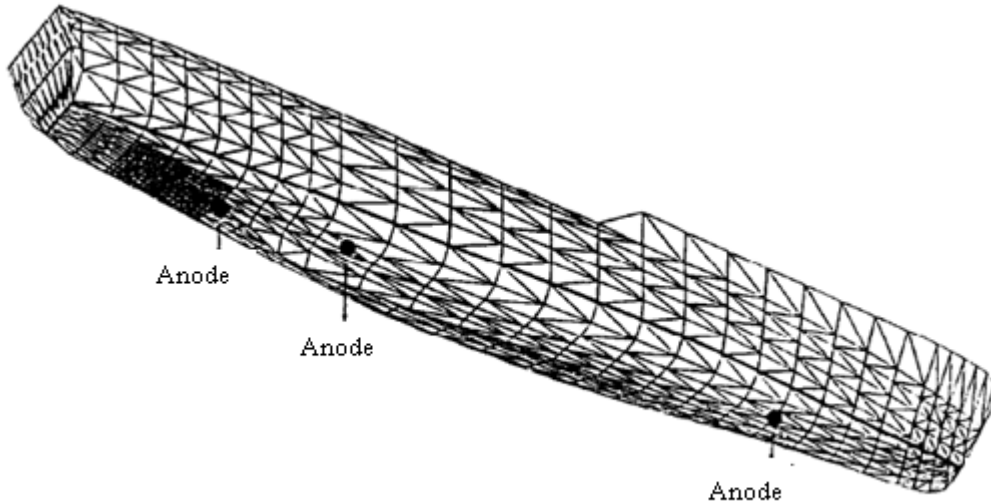
Fig. 2.6 The geometry of Ship [Sun, 1996].

On the other hand, another research [Rannou, 2006] used commercial software (PROCOR) to optimize the design of cathodic protection system of military ships with electromagnetic silencing tools that minimize the electrical field in water to optimize the protective potential. Moreover, Boundary Element Method was used to discover the state of the coating on the ship's hull. This can be done by addressing the areas that act as sink of current. This technique can be used as Non Destructive Test for the coating condition while the ship is in service [Santana-Diaz, 2005B]. DeGiorgi et al [DeGiorgi, 1992] have been evaluating the existing Impress Current Cathodic Protection (ICCP) system conditions on a US navy ship. The software used in this work was BEASY-CP. Similar trends were found in the experimental and computational results. Finally, the physical scale factor that affects the modeling of a ship's cathodic protection was studied [DeGiorgi, 1998]. Physical scale modeling of experimental results is used as the basis for evaluation of a model's accuracy.

Ship Propellers

The propeller is one of the trickiest parts to polarize because it is made from an alloy that contains different elements such as nickel, aluminum and bronze. The shape of the propeller has significant effect on the simulation of cathodic protection. An interesting work [DeGiorgi, 2005] has been done to study the effect of the propeller shape on the cathodic protection simulation. Three methods are used. Boundary Element Method to solve the model assumed that the three shapes of propellers. Discs are used in the first case. The second case used details model for the propeller including individual blades. In the third detailed approach, a propeller is modeled as a solid that is shaped to simulate the complex geometry of a rotating assembly. The results show that addition of more detailed modeling of the propeller results in a decrease in overall system current of 3A only, from 651A to 648A. The addition of shaft geometries did not cause any further reduction in the power requirements.

2.3.1.2 Floating Production Storage and Offloading (FPSO)

The floating units are used in the offshore industry. Many of these systems are converted tankers, or are newly built ships based on modified tankers. In the design stage of the FPSO, it is important to consider the limited possibility of coating maintenance offshore, the required size of anode shielding, and the hydrogen embitterment of structure steel. Osvoll et. al. [Osvoll, 2004] also confirmed that the computer modeling is an excellent tool to evaluate the impress current for this unit because it helps decide the size of shielding and the number of anodes and helps detect any dark spots. They have used a commercial program based on Boundary Element Method (SEACORR/CP) to simulate the FPSOs CP system with different

anode arrangements. Another work for galvanic anode cathodic protection design for FPSO hull has been done [Surkein, 2004]. In that case, the Boundary Element Method was used to confirm that the galvanic cathodic protection is suitable for this application.

2.3.1.3 Offshore oil structures

The protection of offshore structures against corrosion is quite important in oil and gas industry. One of the first modelings of the offshore structure has been done by Strommen et al. [Strommen, 1987]. They also developed a physical model. The results of this work were very promising in the field of cathodic protection modeling. After 15 years of working in computer modeling of offshore CP system, Gartland et al [Gartland, 1999] concluded that Boundary Element Method is a very convenient basis for CP modeling. The computer modeling of cathodic protection on risers or tendons expands the use of CP simulation to consider the metallic tension legs of a platform where anodes are mounted on the hull or subsea structures. A commercial CP simulation was used to perform a parametric study to identify the limitations of CP and coating that provides corrosion protection. The effect of using titanium riser instead of steel riser was also considered. The result shows that the computer simulation is very useful in analyzing such problems. [Osvoll,1995].

A modern and interesting research on the application of cathodic protection simulation of a chain connector which is a few meters long pipe fully immersed in seawater with the ratchet on buoy side and the guide ring on the other side. A few links of chain located inside the pipe must be cathodically protected from sacrificial anodes which can only be located on the external part of the hawse. The space between chain links and internal part of the pipe is narrow, resulting in a significant potential drop. To insure current distribution on the chain,

holes have to be drilled on the pipe so that more cathodic protection can reach the surface of the links. The program successfully modeled these critical parts. [Roche, 2008]. A research group in Italy studied the application of Boundary Element Method to offshore cathodic protection modeling using BEASY commercial software. Their results proved the calculation program was accurate for various geometrical configurations [Cicognani, 1990].

2.3.2 Pipelines

The protection of pipelines from external corrosion is commonly accomplished by the combination of pipeline coating with cathodic protection, which protects those portions of the pipelines that are inadequately coated or where the coating contains problems. The defects in the pipeline coating that expose bare steel are termed "holiday". The conventional anode resistance formulas that ignore the current and potential distribution on the pipes are inadequate for modeling pipelines with holidays. Current and potential distribution must also be considered when modeling multiple pipelines [Adey, 2000A]. In this paper different cases of pipelines CP system were modeled with various types of coating which show how flexible the modeling is. On the other hand, computer modeling can be used to aid traditional cathodic protection design method for coated pipelines [Degerstedt, 1996]. Earlier research was done in 1994 to numerically model the cathodic protection for buried pipeline. The mathematical model was based on Boundary Element Method and Finite Element Method. This approach assumes that the soil was homogeneous, and local earth surface was presumed flat. The results showed simplification of macroscopic design with the information of potential levels along pipes, potential distribution in the soil, axial currents flowing through pipelines. The comparison between measurements and numerical results was successful, with maximum error of 15% [Brichau, 1994].

Orazem et al. [Orazem, 1997] also used the mathematical method (Boundary Element Method) to model cathodic protection underground pipeline with holiday coatings. The performance of a parallel-ribbon sacrificial anodes CP system for coated pipelines was assessed. In the cases studied, magnesium ribbons provided adequate protection in 50 KΩ-cm soil resistivity, but almost no additional protection was achieved by retrofitting Mg anodes to a CP system using zinc ribbons if the zinc ribbons remained connected to the pipe. Orizem et. al.'s study also showed the lack of sensitivity of above-ground on-potential surveys displaying localized corrosion on the buried pipe. In Malaysia, ribbon sacrificial anode was used also to protect the pipeline structures [Safuadi, 2008]. This particular cathodic protection system was evaluated using 2D boundary element method. It has been found that the current density values on the surface of the pipe are subject to change when the factors such as soil conductivity, material of the anode, and displacement between pipeline and anode [Safuadi, 2008]. Moreover, a very interesting study was conducted to simulate the cathodic protection system for a buried pipe segment using 3-D Boundary Element Method. A U –shaped vault of infinite resistivity was positioned upside down over this pipe segment for mechanical protection purposes such as the road crossing. Fig.3.7 shows (a) triangular grid for the U-shaped one-domain triangular; (b) sketch of the two-domain model with the first domain indicated in gray and the interfaces with the second domain being surfaces 1,2 and 3; (c) two-domain triangulation. The electrical obstruction effect was investigated. To limit computational efforts, two ring-shaped defects were considered on the pipe surface. The protection level of both defects was compared for different values of soil conductivity. The pipe coating is considered to be non ideal with 1% defect of total surfaces. The model was successfully solved. As a result, when a U-shaped

vault is present around a pipe segment, the impact on the protection level of defects that are positioned under the vault becomes important for low conductivity soils ($\sigma = 0.01$ Ω-1m-1 or less). In that case, the CP level might drop by at least 100 mV [Purcar, 2003].
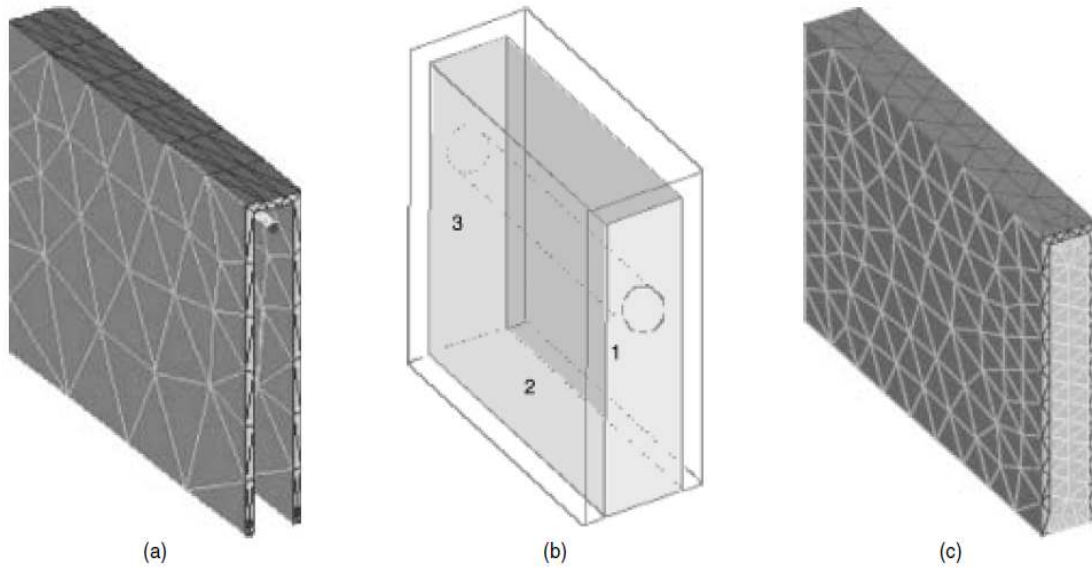
Fig. 2.7 Triangular grid for the U-shaped model [Purcar, 2003].

2.3.3 Storage tanks

The storage tank is usually protected against corrosion by cathodic protection when it is in contact with electrolyte (internally) or with soil (buried or above ground):

2.3.3.1 Above- ground storage tanks

Storage facilities for petroleum products usually consist of a collection of above ground storage tanks called a tank farm. The tanks are cylindrical in shape, are constructed of steel, and rest on the soil. The tank bottom, then, is subject to the same corrosion as are buried pipelines. As the tank bottom is supported by the ground and is subjected only to hydrostatic

pressures, the bottom of tank can be made of thinner metal than what is used for pipelines, which are exposed to all around pressure. Because the metal is thinner at the bottom, it can be more easily perforated by even low rates of corrosion. While the primary current distribution on the pipes is uniform, the primary current distribution for the circular area of the tank bottom is inherently non-uniform. "Limitations of kinetics and mass-transfer may cause the distribution to become more uniform; nevertheless, the tendency toward a non-uniform current distribution compromises delivery of protective current to the center of the tank bottom" [Riemer, 2005]. The final issue constraining design of cathodic protection systems is that the concentration profiles for oxygen under a storage tank are cyclic in nature. The principle cathodic reaction on the tank bottom is usually assumed to be reduction of oxygen. When the tank is filled, the bottom of the tank is in full electrical contact with the soil, allowing reduction of oxygen. Eventually the consumption of oxygen reduces the oxygen content of the soil under the tank. When the tank is empty, the center rises above the soil creating a void. The resulting bellows action replenishes the oxygen content in the soil. The mass-transfer-limited current density for reduction of oxygen must therefore be considered to be a function of both time and position. All these issues make the simulation of a storage tank critical. Riemer [Riemer, 2005] has developed a mathematical model for the tank bottom. A single tank was modeled for which protection was provided first by an anode located far from the tank bottom, second by a series of anodes distributed around the circumference of the tank, and third by an anode grid laid directly underneath the tank bottom. Riemer considered two cases for each anode location. The first case considers uniform oxygen concentration, to approximate the initial conditions when the tank is first filled, while the second is based on the calculation of oxygen concentration. The results

demonstrate that assumption of a uniform current distribution on the tank bottom, used previously, was found invalid. The ribbon anodes installed underneath the tank seem to be a effective solution to protect the tank bottom [Riemer, 2005].

2.3.3.2 Buried tanks

A buried tank is smaller than above ground storage tank. It is usually protected by sacrificial anodes (magnesium or zinc). A group from France used the finite element method to model the cathodic protection of buried tanks. They studied different parameters that influence the CP design such as the electrical conductivity of the soil and the quality of the tank coating. The result showed that 2-D modeling can obtain a fairly precise description of the 3-D performance of a buried tank. [Rabiot,1999]. A similar work by Aboobtalebi et al. studied the sacrificial cathodic protection. The tank was protected by zinc anode and the mathematical technique used the Boundary Element Method for modeling the CP system. They had found that the simulation is a useful tool in the design of cathodic protection. [Aboobtalebi, 2010]. The cathodic protection for a storage tank was simulated successfully by Boundary Element Methods with genetic algorithms.

2.3.4 Simulation of the well casing

Cathodic protection is often employed to prevent external corrosion of oil production well casing. It is known that the total current required to protect a casing cannot be predicted with any certainty, nor can surface measurements alone determine the level of protection at the bottom of the casing. The actual protection level along the well bore can be directly measured with special tools, but this is expensive both in direct cost and in lost production. An efficient Boundary Element Method was developed to study the cathodic protection of

the well casing in a formation with layered conductivity [Lee, 1993]. The Newton-Raphson technique as a numerical method was used to satisfy the nonlinear boundary condition [Lee, 1993]. Simulation results confirmed a weak dependency on the azimuthal direction of the current distribution on the well casing. The maximum current occurred at the top of the well casing and the current density gradually become smaller along the axial direction; the same is found in actual measurements [Lee, 1993]. The simulation technique has been used to check the possibility of utilized unused well casing as anode for cathodic protection system to protect other new well casing. The result gives a promising means for having a quasi-uniform distribution of the current density profile along the protected well casing axial length with low current density requirement of the anode [Metwally, 2008].

In this chapter the examples of the cathodic protection application have been provided. However, other issues of cathodic protection such as stray current interference, optimum location of anodes and influence of coating, remain problematic in the real life applications.

2.4 Issues associated with modeling of cathodic protection

2.4.1 Cathodic protection interference

Cathodic protection interference and stray current are serious problems in the cathodic protection field. One ampere of DC current discharge from the pipeline for one year may consume 10 kg of steel. The unprotected structure is picking up the current (Pick up point) on one side and discharge the current (Discharge point) on low resistivity side. Severe corrosion occurs on the discharge point.

There are four types of the CP interference:

1) Anodic Interference

 The unprotected structure is located on the potential gradient of the anode of another CP system. The interference would be worst if the unprotected structure is closer to the anode Fig.2.8.

2) Cathodic Interference

If a badly coated pipeline crosses the zone near a cathodic protection structure, the interference might exist as Fig. 2.9.

3) Combined Interference

In this case, a foreign pipeline is passing through the anode potential gradient area and also crossing the protected structure. The interference takes place on two parts of the foreign pipeline close to both anode and cathode as in Fig. 2.10.
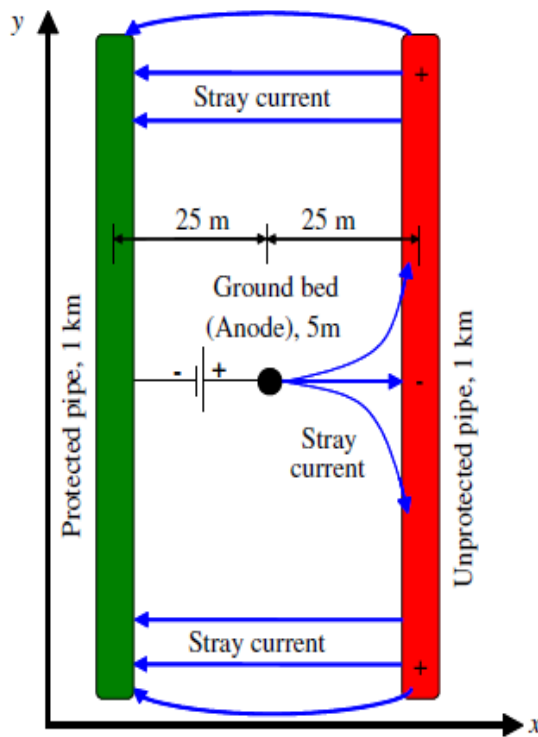
Fig. 2.8 Anodic Interference [Metwally, 2007]   **Fig. 2.9** Cathodic Interference [Metwally, 2007]
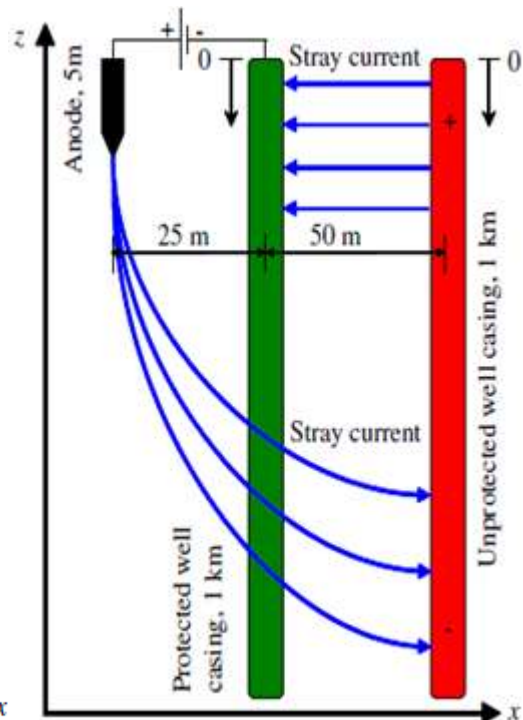
27

4) Induced Interference

Fig.2.11 shows that induced interference happens when two unprotected foreign structure (1 & 2) passing close to a cathodic protection system. The structure 1 will pick up the current because it is closer to the anode bed and discharges the current to the other structure 2. Next, the structure 2 picks up the current from 1 and discharges the current close to the cathode in the cathodic protection. This is very dangerous, and it happen frequently in the industry.
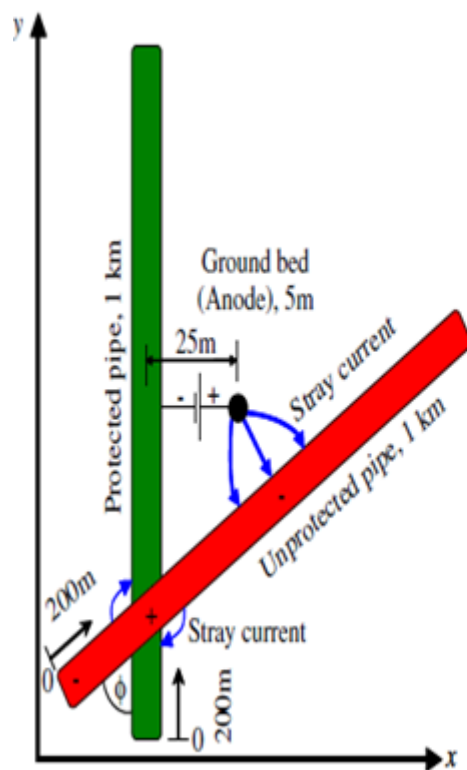
Fig. 2.10 Combined Interference [Metwally, 2007]   **Fig. 2.11** Induce Interference [Metwally, 2007]
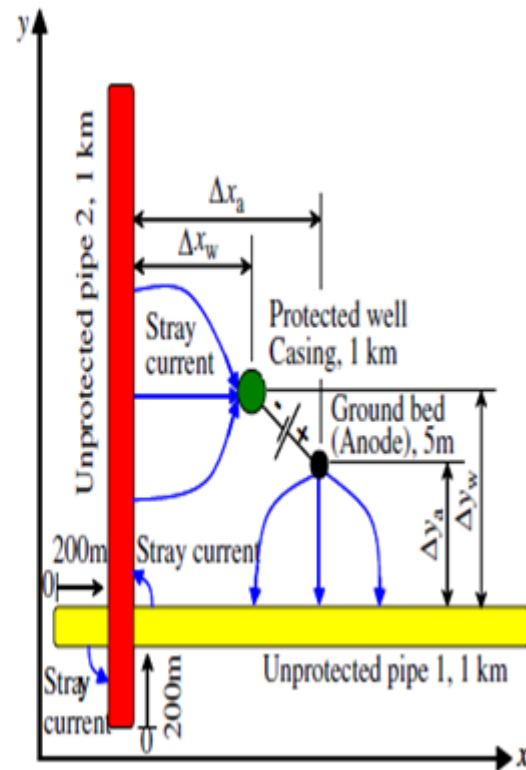
Cathodic protection interference problems/types are simulated. The modeling method used boundary element method based BEASY software to model the different types of the interference. Metwally et. al. had found that the software is very flexible and effective to

predict the CP interference. The software was found to be very flexible and easy to perform simulation for cathodic protection, it's effective to predict the CP interference [Metwally, 2007].

Early work has been done by Brichau et. al [Brichau, 1996]. A new numerical method was created to simulate the interference. The name of this method is OKAPPI and they concluded that the result was accurate. They had found that the software is very flexible and effective to predict the CP interference. More types of interference (e.g. railway interference) were added in the study. In addition, the simulation of stray current corrosion between the ship and the piles can be made by using Boundary Element Method [Trevelyan, 1994].

2.4.2 Optimum location of the anodes and reference electrode

The design goal of the cathodic protection system is to produce an evenly distributed protection potential on the structure as well as to reduce the power consumption of the anode to a minimum. The available conventional design will calculate the number of anodes needed and assume the location of reference electrode and anodes. The constraints on the design are the values of the potential on the structure. In order to provide adequate protection, the potential must be less than a specified value (e.g. -850). The potential must be greater than a specified value (e.g. -1200) to prevent over-protection. The best location of the anodes and reference electrode can be chosen by simulation. By combining an automatic optimization procedure with the Boundary Element Method model of the ICCP system, an optimum solution can be obtained. Boundary Element Method has been used to select the optimum locations for anodes on the ships, storage tanks and underground pipeliness [Adey, 2000]. The same approach was used to reach the uniform distribution of the cathodic protection

potential by changing the position of the anodes along the ship body. The simulation is a perfect tool to show the optimum location of the anode and reference cell [Rannou, 2006]. As mentioned before in page 16, Sun studied the possibility for optimum control of impress cathodic protection systems in ship building. He had used the Boundary Element Method to model the system. The number of anodes increased to achieve the uniform distribution. [Sun, 1996].

Optimizing the location of anodes in cathodic protection systems to smooth potential distribution was done. The anode has been moved to increase the symmetry of the potential on the damages area with satisfactory results. The symmetry of the potential of the damaged area was studied and the final values of the optimization process were validated by the results of a scan over the whole search area. [Santana, 2005 A]. Recently, the Boundary Element Method along with Matlab program was used to select the best location of the anode for a sacrificial cathodic protection of a tank [Abootalebi, 2009].

On the other hand, the Boundary Element Method was used to optimize the location of the reference electrodes in the cathodic protection system. The problem is reduced to minimizing the power supply under the protection conditions which are taking into account by some different scenario. First, the cathodic protection system where the electrodes have to be located directly on the wall of the structure is considered. Next, the cathodic protection system where the electrodes are located in the electrolyte is considered. The location of the electrode has been modified. The optimum current to be impressed to each electrode has to be determined. [Aoki, 1997].

2.4.3 The influence of coating

Cathodic protection system is usually used in conjunction with organic coatings on the pipelines and other metallic structures to provide protection in regions with the coating damages. These systems mitigate the corrosion at exposed metal surfaces. The coating in the cathodic protection plays a major role in the accuracy of the modeling. DeGiorgi [DeGiorgi, 2002] has investigated the assumptions of the perfect painting in the modeling of cathodic protection. This is a simplified assumption that facilitates computational modeling. The appropriateness of this assumption for analysis of real shipboard systems has been questioned. Physical scale model was used for comparison. The result shows that paint with a relative polarization response of 0.1 or greater (paint effectiveness, 0=perfectly insulation, 1=bare steel) exhibits significant difference in calculation and it can't be modeled as perfectly insulating materials.

Moreover, the effect of coating integrity on the impress current cathodic protection system was one of the areas that have been studied. DeGiorgi found that the electrical current requirements increased due to damages in the coating [DeGiorgi, 1995].   Nevertheless, the pipelines with holiday coating are easy to be recognized using the cathodic protection simulation because they appear like a sink of the current. To prove that pipelines with perfect and poor coating have been modeled, the pipes with coating surfaces can be modeled in several ways. The coating can be considered to be a perfect insulator, a highly resistive barrier to current or a selective barrier to ionic transport, allowing water, dissolved gases and ionic species to permeate through the pipe. The effect of stray current between multiple adjacent pipelines or with holiday in the coating of the straight pipeline was determined. The

simulation of the cathodic protection was very useful to deal with these issues [Adey, 2000A].

Damages often appear on the hull of a vessel during its lifetime. In many cases, the locations of damage are unknown. The simulation was also used to predict the coating condition of the ship. The number of the reference cell was increased to determine how much data was required to detect the damage. Data from the corrosion related electric and magnetic fields can also be employed to identify the condition of the vessel. [Santana-Diaz, 2006].

The final issue regarding modeling of the cathodic protection with coating is the cathodic protection under a delaminated coating. This issue was addressed by Allahar and Orazem. A mathematical model was presented for the steady-state condition in a delaminated region surrounding a circular holiday on a metal surface under cathodic protection. The linearized governing equations for species mass-transfer and electro neutrality were discrete using second-order difference. Oxygen reduction and distribution normal to the metal surface were found to be negligible for delaminated region more than 3 cm. The result demonstrated that the commonly employed assumption that concentration gradients are negligible is not valid within the delaminated region. [Allahar, 2009].

Chapter 3

Experimental aspects

3.1 Sacrificial cathodic protection

The objective of this section is to apply modeling technique in the sacrificial cathodic protection. This can be achieved in a three-part process. In the first part, a simple cathodic protection sacrificial experiment was modeled with a single anode and a cathode. In the second part, another type of cathode was added (either copper or high silicon cast iron). Finally, an actual CP system inside a storage tank was simulated to determine the root cause of the failure of the magnesium anode in the CP system.

3.1.1 Single cathode and single anode

Objective

This experiment was conducted to test and learn the capabilities of BEASY CP software in the protection of a mild steel sheet, using pure zinc as the anode of this sacrificial CP system.

Introduction

A simple sacrificial experiment was conducted using a mild steel sheet as the cathode and pure zinc as an anode, both of which were immersed in synthetic ground water.

Materials

- Cathode: a mild steel sheet with the dimensions of 25.4 cm x 15.24 cm and 453.7 grams

- Anode: a zinc bar with 20.5 cm in length, 1.25 cm in diameter, and 175.6 grams.

Electrolyte

The experimental container held synthesized simulated ground water with chemical composition found in Table 3-1. The initial conductivity of the electrolyte was 2.6 S/m. After six months, the conductivity increased to 4.2 S/m.

Table 3.1 Chemical compositions of the synthesized ground water.

Element	Composition (g/L)
Chloride, Cl	9.24
Sulphate, SO4	2.700
Bicarbonate, HCO3	0.107
Bromide, Br	0.055
Fluoride, F	0.0004
Sodium, Na	5.3296
Magnesium, Mg	0.8779
Potassium, K	0.2687
Calcium, Ca	0.183

Experimental Procedure

In performing this experiment, the cathode and the anode were immersed in an electrolyte and then the natural potentials of the cathode and the anode were measured before being connected to a standard calomel electrode (SCE) positioned in the middle of the container. After that, the cathode and the anode were connected through external shunt resistance (R=0.001 Ω). Next, the protection current started to flow from the zinc to the steel sheet, causing potential polarization in the steel sheet. A fresh synthesized ground water was

continuously fed in at a flow rate of 0.9 L/min. Fig. 3.1 shows a schematic of experimental

setup and Fig. 3.2 is a photograph of the lab setup.
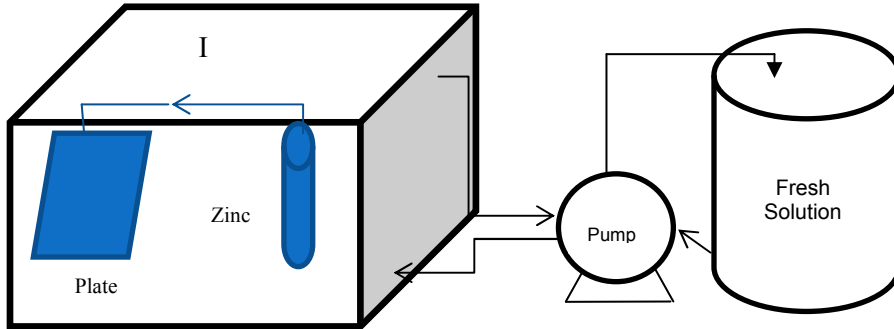
Fig. 3.1 Schematic illustrating the experimental setup.

Fig. 3.2 Photo of the experimental setup.

3.1.2 Two cathodes and single anode

Objective

To observe the current drainage using experimental and simulation technique, two different

materials were connected to a single sacrificial zinc anode.

Introduction

As an extension of the first section, the same experimental setup was used to test current

drainage. A copper rod was connected to the steel sheet and then it was replaced by a high

silicon cast iron (HSCI) rod as the current was observed. The electrolyte composition was the

same as those in the first section.

Materials

- A pure copper rod with the following dimensions, d = 0.762 cm, l = 21.5 cm, Area= 52.38 cm^2

- The HSCI rod with the following dimensions, d = 1.27 cm, l = 21.5 cm, Area= 88.3 cm^2. The HSCI, whose chemical composition accords with the international standard (ASTM A 518 Gr3) as listed in Table 3-2, was supplied by Anotec manufacturers.

Table 3.2 Chemical Compositions for HSCI

Standard	ASTM A 518 Gr3	
Elements	Minimum (percent in weight)	Maximum (percent in weight)
Silicon	14.20	14.75
Chromium	3.25	5
Carbon	0.70	1.10
Manganese	0	1.50
Molybdenum	0	0.20
Copper	0	0.50

Experimental Procedure

A copper rod was connected to the mild steel sheet directly both of which were connected to the zinc anode through an amp. meter to measure the current. The circuit was connected for 24 hours. The copper rod was replaced by an HSCI rod and the same steps were repeated.

3.1.3 Application of internal sacrificial cathodic protection

Objective

The object of this experiment was to investigate the reasons for the failure of magnesium as an anode for the sacrificial cathodic protection system in a high- alkaline solution. An aluminum alloy anode which replaces the magnesium anode was also studied in the same electrolyte.

Introduction

Pitting corrosion has been observed in the interior of a tank after only three years of service in one of the SABIC petrochemical plants. The tank was supposed to be protected by sacrificial magnesium anodes suspended from the roof. In this work, the investigation of the magnesium anode was accomplished in two phases: first, in a study of the corrosion behavior of magnesium in the same environment using a potentiodynamic technique and then, second, in the modeling of the sacrificial system through a BEASY cathodic protection simulation. The same test was performed for the aluminum alloy that was used to replace the magnesium.

Materials

Magnesium: pure magnesium was supplied from a local cathodic protection company.

Aluminum Alloy: a Galvalum III anode alloy that is normally used in the cathodic protection systems of ships was supplied by Purity Casting Alloy Company, with the chemical compositions in Table 3-3.

Table 3.3 Galvalum III chemical compositions.

Element	Percentage in Weight
Fe	0.13 max
Zinc	2 - 6
In	0.01 – 0.02
Si	0.08 – 0.2

Electrolyte

The storage tank's contents were composed mainly of potassium carbonate K_2CO_3, along with other elements in low concentrations, as shown in Table 3-4, below, which gives the chemical analysis of this solution:

Table 3.4 Chemical analysis of the tank solution.

Parameter	Unit	Value
Chloride	mg/L	0.12
Phosphate	mg/L	220
Sulfate	mg/L	440
Sodium	mg/L	450
Potassium	%	15.9
Magnesium	mg/L	15.8
Calcium	mg/L	39
TDS	mg/L	160165
pH	-	10.5
Conductivity	mS/cm	145

3.2 Impress current cathodic protection

3.2.1 Simulation of pipe segment

Objective

The objective of this test was to apply BEASY software to simulate impress current system and to learn how to deal with the available functions.

Introduction

A small section of carbon steel pipe is protected by high silicon cast iron anode that is connected to an external DC power supply. Both cathode and anode are buried in sand soil.

Materials

Cathode

Carbon steel pipeline with 60 cm in length and 6.33 cm in diameter. The wall thickness is 0.293 cm.

Anode

A bar of high silicon cast iron with 33 cm in length and 2.732 in diameter. The chemical analysis of the anode as per ASTM A 518 Gr3 is provided in Table 3-2.

Electrolyte

The electrolyte is represented by sand brought from the area that is close to one of the Vancouver beaches. The resistivity of this sand is very high and was measured by a method called Four Pens Method. The procedure of this method is simply to apply direct current to the two ends of the container and measure the potential in-between.
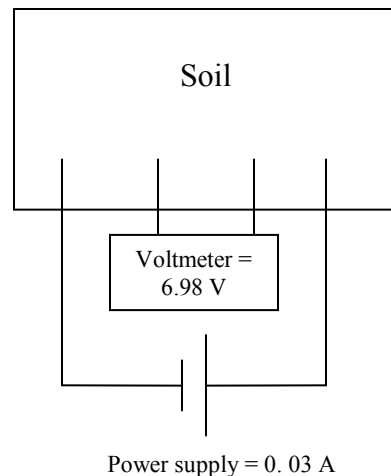

Fig. 3.3 Four Pin Method to Measure the Soil Resistivity.

As illustrated in the previous Figures 3.3, 0.03 Amp current was applied to the outer pins while the voltage measurement in the internal pins was 6.98V. The conductivity can be calculated as follows:

$$R = \frac{6.98}{0.03} = 232.66\Omega$$

$$\rho = 2\pi l R = 29237 \ \Omega\text{-cm},$$ Where l is the spacing between the pins and equal 20 cm.

$$k = \frac{1}{\rho} = 3.42 x 10^{-5} S/cm$$ k is the conductivity

The purpose of measuring the resistivity is to know the electrolyte condition and to use measured resistivity later in the BEASY software.

Experimental Procedure

1- The carbon steel pipe has been buried in the soil (Fig. 3.4) and the natural potential was taken between the pipeline surface and the copper/copper sulfate (Cu/CuSO$_4$) reference electrode (Fig. 3.5).

Fig. 3.4 Lay down of the pipeline in the soil

Cu/CuSO$_4$
Reference
Electrode

Fig. 3.5 Natural potential measurement of the pipe.

2- In this step, high silicon cast iron anode was connected to the positive pole of the DC power supply, and the carbon steel pipe was connected to the negative side. The DC power supply was maintained to feed 1mA to the anode though the connecting to high resolution ammeter as in Fig.3.6.

3- The potential of the cathode was taken by Cu/CuSO$_4$ reference electrode which was fixed above the pipe.
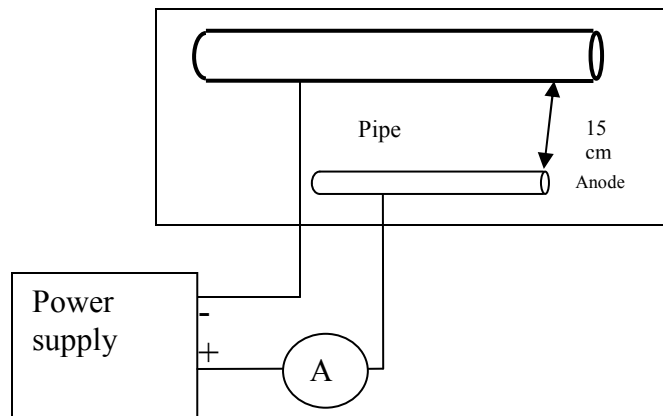

Fig. 3.6 Schematic diagram of the pipe segment experiment.

3.2.2 Application of impress current design

Actual design was created to protect 12 parallel pipes with 6 anodes distributed around the pipelines. The length of each pipe is 33.3m and all the pipes are located on the utility side of petrochemical plant to transport gases, water and raw materials e.g. ethylene. The design takes into account that each anode produces maximum 2 ampere. This can be noticed as the selected transformer rectifier rate (12 ampere/ 12 Volt). Fig.3.7 shows schematic for the proposed design while Table. 3-5 provides the diameter for each pipe.
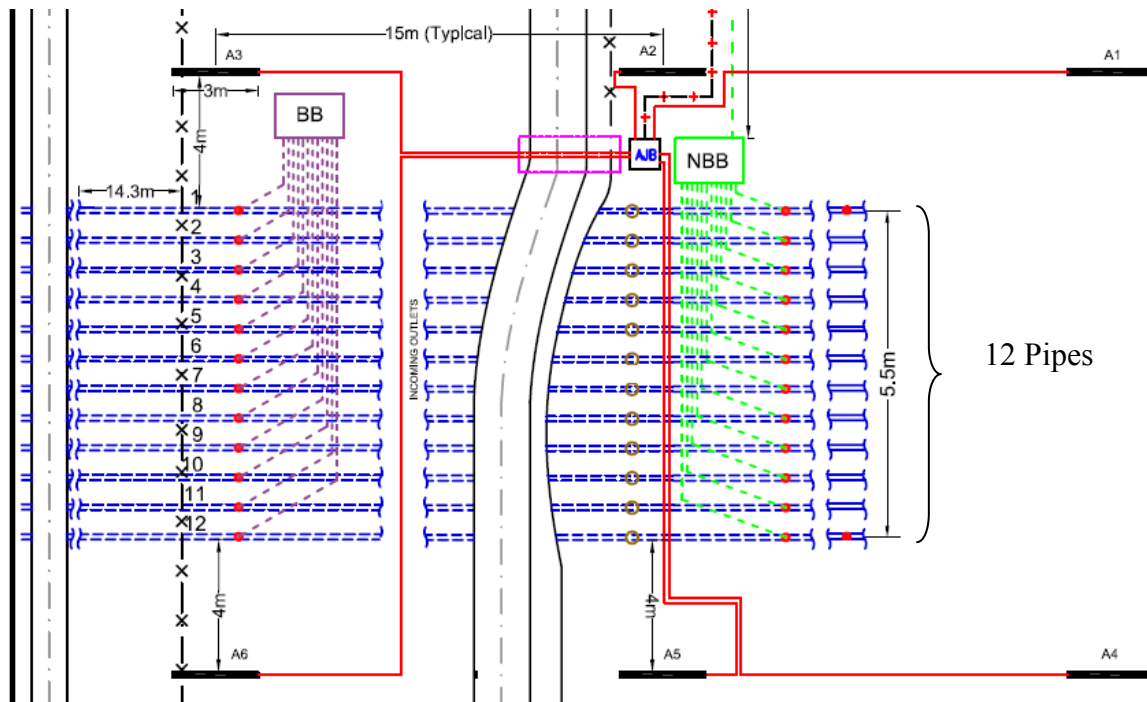

Fig. 3.7 Schematic illustrates the pipes and anodes position.

Table 3.5 List of pipes diameters.

Pipes Number	Pipe Diameter (cm)
1	20.32
2	7.62
3	5.08
4	5.08
5	25.4
6	7.62
7	10.16
8	10.16
9	7.62
10	7.62
11	15.24
12	25.4

3.3 Potentiodynamic test procedures

Throughout the experiments of this research, all electrochemical tests were conducted at the ambient temperature (except for section 3-1-3 which was in 60 ^{0}C) and under atmospheric pressure. Tests were conducted using standard glass cells containing the working electrode (material that shall be tested) and a graphite counter electrode. The reference electrode was

Saturated Calomel Electrode (SCE) that interfaces to the test solution via a salt bridge that terminated about 2 mm from the working electrode.

VersaSTAT4 potentiostat system was used to perform and analyze the Potentiodynamic polarization curves. The system was controlled by the VersaStudio software package.

After preparing the solution and pouring it into the electrochemical cell, the tested material was immersed in the test solution for 60 minutes in order to measure the open circuit potential (E_{OCP}). E_{OCP} measurement was made between the working electrode and the reference electrode while no current was passing through the working electrode. The objective of this test was to find the potential at which the anodic and cathodic reaction currents at the working electrode and solution interface were balanced. Moreover, the E_{OCP} measurements were needed prior to the electrochemical polarization tests to insure potential stability.

Once the open circuit potential (E_{OCP}) stabilized, at approximately 60 min interval the electrode potential was swept potentiodynamically at a scan rate of 0.1667 mV/sec. All potentials in this test were measured with respect to the Saturated Calomel Electrode (E = 0.241 V vs. standard hydrogen electrode SHE).

Chapter 4

Computer modeling

The computer modeling was done using BEASY simulation software. There are three major stages in BEASY software:

1- Model preparation

This stage involves the definition of the geometry and the environmental conditions. The geometry is described by subdividing the boundary of the problem (the surface of the structure and anodes in the case of CP) into a number of elements inter-connected at nodes. The nodal coordinate and element conductivities are defined. The size and type of elements are chosen according to the complexity of the problem and the order of the approximation required describing the variation of voltage or current density over the surface of the elements. The geometry model can be set up using GiD drawing program.

2- Simulation

The computational scheme assembles the boundary element equations representing the electrolyte and couples them with the equations derived from the polarization data. The set of equations is then solved iteratively and the values of current density and potential, computed at the boundary nodes. If time dependent polarization data is defined the conditions at the nodes is predicted at different times as requested by the user.

3- Post Processing

At this stage the result obtained can be viewed graphically by the use of post-processors. These modules can be used interactively to create:

I. Graphic display of the mesh or a solid model of the geometry with various distributions of the anodes under consideration.

II. Solid or line color contour plots of the voltage and current density distribution.

III. Close-up viewing of both the geometry and the results at areas of interest.

IV. Plots of the variation of the voltage or current density with time at a particular position.

The following flow chart illustrates the basic stages for the BEASY program:

1- Read input
   ▪ Define Geometry.
   ▪ Discretise geometry (Mesh generation)
   ▪ Constraint equations

2- Simulation:
   ▪ Compute BEM integrals H and G
   ▪ Assembly of $A\ X=B$ (by applying boundary conditions)
   ▪ Solve $A\ X = B$

3- Post-process results
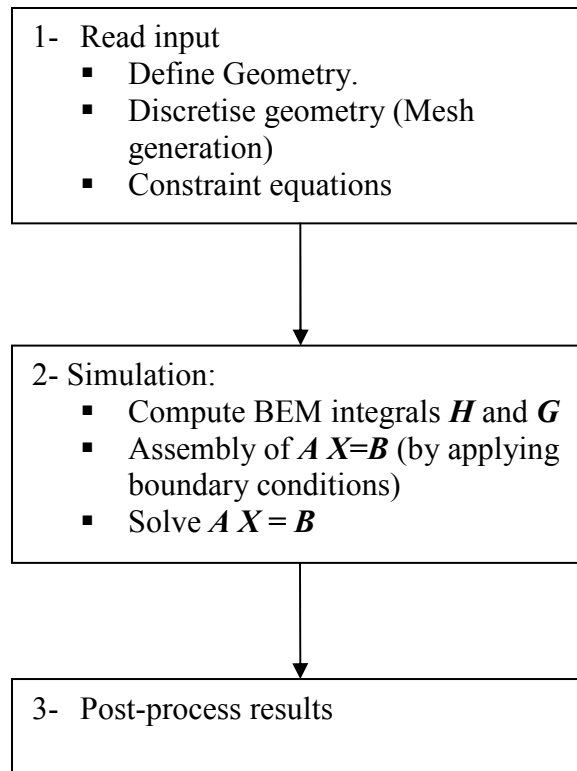
Fig. 4.1 Flow-chart for the BEASY process basic steps [BEASY, 2009].

Boundary Conditions

The polarization behavior on the surface of the cathodes and anodes is described by the definition of boundary conditions. The boundary conditions can take the form of constant voltage, constant current (impress current anode) or linear or nonlinear relationship between the voltage and the current density. The nonlinear relationship can be used to simulate the real polarization taking into account the effect of environmental conditions.

4.1 Sacrificial cathodic protection

4.1.1 Single cathode and single anode

Defining the geometry

The geometry of the model was built in GiD drawing software. GiD is a drawing tool that works as an interface between the model and the BEASY solver software. Fig4.2. illustrates the geometry of this experiment.
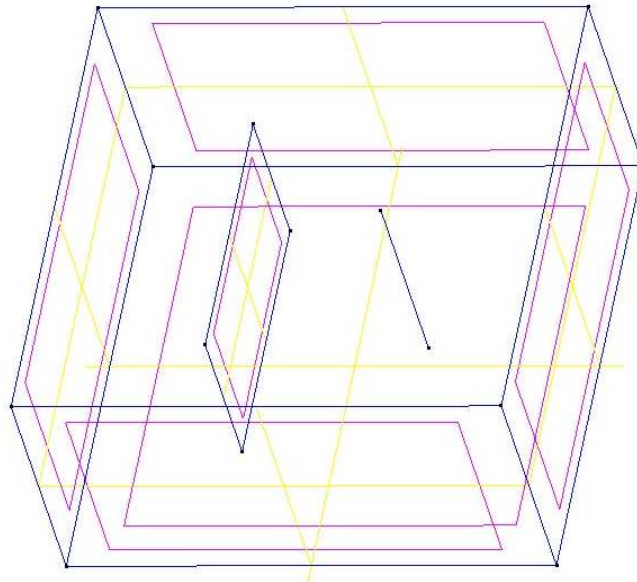

Fig. 4.2 Geometry of the single cathode and single anode experiment.

Once the geometry was ready, the groups (units, zone or electrolyte, tubes, symmetry and polarization material) were defined.

Mesh generation

The meshing was generated as the following Fig. 4.3 that separated geometry into 710 elements.
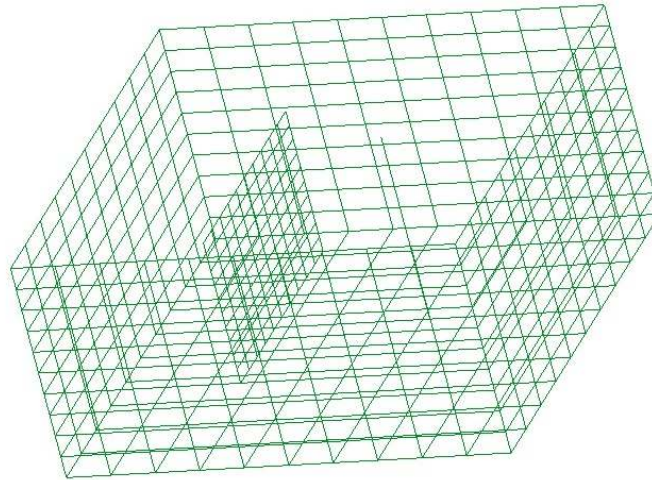

Fig. 4.3 Meshing generation for single cathode and single anode model.

Boundary conditions

The values of the potential and current density of the potentiodynamic curves (Fig.4.3 and 4.4) were inputted into the BEASY material database to solve equation (18) in Chapter 2, Section 2-2-3 which will be used to form the matrix equation (19). Then the simulation will follow the flowchart in Fig.2.3 in Chapter 2. For the zinc, the potential and current density of the anodic behavior in Fig. 4.4 were inputted.
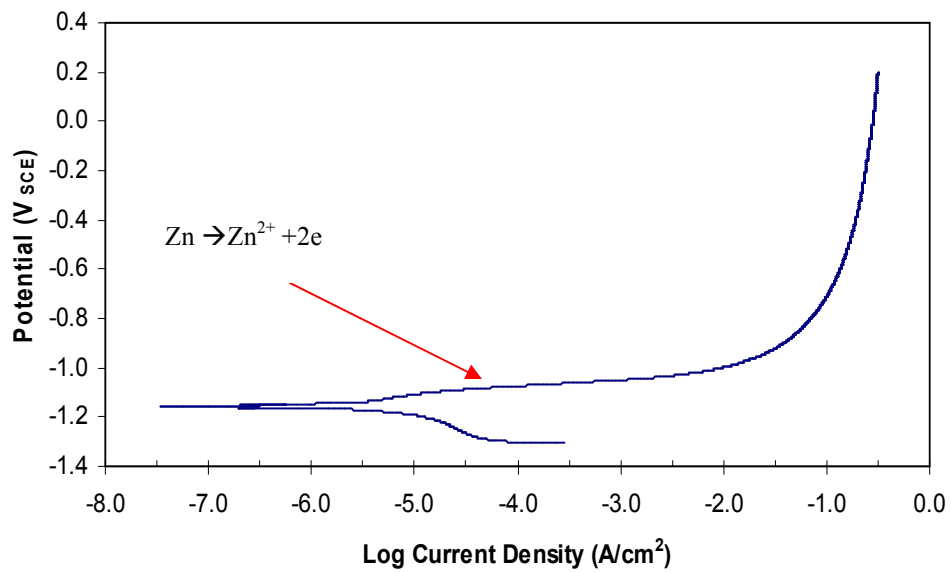
Fig. 4.4 Polarization curve of zinc anode with 0.1667 mV/sec scan rate and ambient temperature under atmospheric pressure.
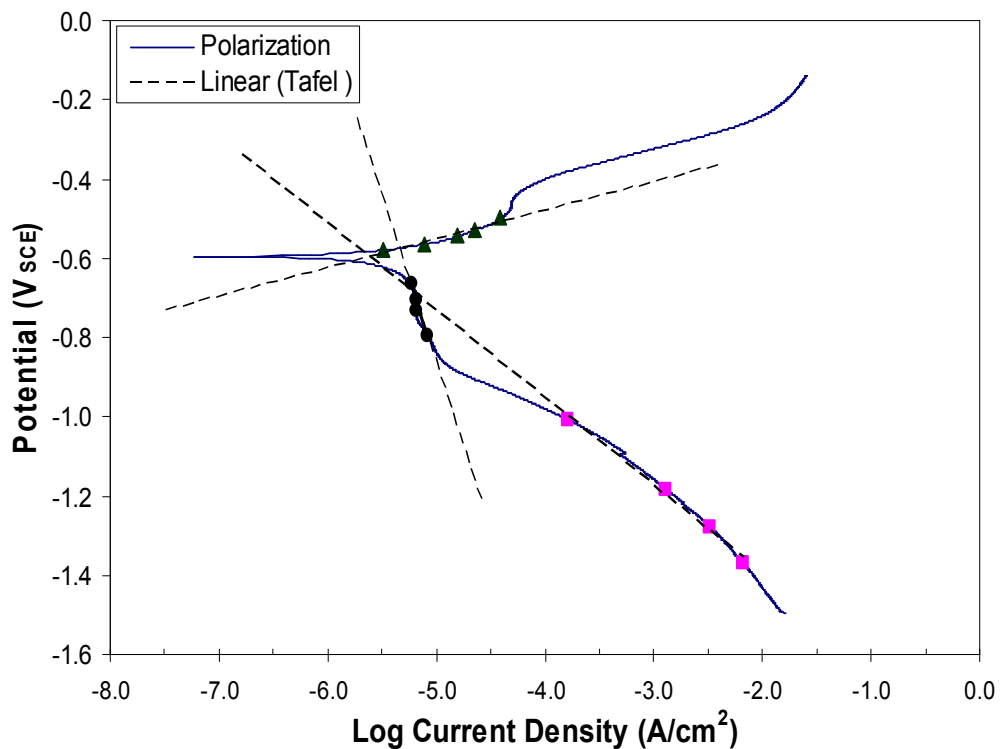

Fig. 4.5 Polarization curve of mild steel with 0.1667 mV/sec scan rate and ambient temperature under atmospheric pressure.

Figure 4.5 presents the polarization curve of steel which is associated with three half cell reactions occurring on the surface as follows [Abootalebi, 2010]:

$Fe \rightarrow Fe^{2+} + 2e^-$

$H_2O + \dfrac{1}{2} O_2 + 2e^- \rightarrow 2OH^-$

$H_2O + e^- \rightarrow \dfrac{1}{2} H_2 + OH^-$
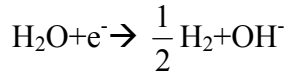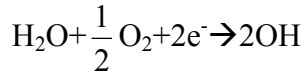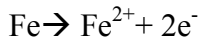
According to the Tafel's law, the following equation can be used for each half reaction [Qiu, 2004]:

$$\eta = c + b \log I \qquad\qquad\qquad\qquad (20)$$

In which η is the over potential, I is current density, b is Tafel slope and c is a constant. By inserting $\eta = E - Eeq$ in Tafel equation it changes to:

$$E - Eeq = c + b \log I \qquad\qquad\qquad\qquad (21)$$

Equation (21) can be rewritten as [Abootalebi, 2010]:

$$i = 10^{\left(\frac{E+\alpha}{\beta}\right)} \qquad\qquad\qquad\qquad (22)$$

In which α and β are constants characterizing polarization curves and:

$$\beta = b$$

$$\alpha = -Eeq - C \qquad\qquad\qquad\qquad (23)$$

In the potentiodynamic polarization measurements of steel, the net current is [Yan, 1992]:

$$I_{net} = I_{a1} - I_{c1} - I_{c2} \qquad\qquad\qquad\qquad (24)$$

Where I_{a1}, I_{c1} and I_{c2} are the current density generated by iron oxidation, oxygen reduction and hydrogen evolution respectively. Therefore the net current in potentiodynamic polarization measurements of steel is [Abootalebi, 2010]:

$$I = 10^{\left(\frac{E+\beta a1}{\alpha a1}\right)} - 10^{-\left(\frac{E+\beta c1}{\alpha c1}\right)} - 10^{-\left(\frac{E+\beta c2}{\alpha c2}\right)} \qquad (25)$$

Using the least square method where $R^2 > 0.95$ to calculate the constant α and β. Applying calculated values of α and β to equation (25):

$$I = 10^{\left(\frac{E+0.0719}{0.2553}\right)} - 10^{-\left(\frac{E+0.8504}{4.2846}\right)} - 10^{-\left(\frac{E+0.2205}{2.233}\right)}$$

This step made the test of the software more reliable, as it used the actual material behaviors to calculate the final results.

Next the model is ready to be saved in the BEASY format. After the file was saved, the BEASY solver program read it and then arranged the material as cathode, anode and electrolyte. The next step was to use the material file identified earlier and then select the conductivity in the experiment and choose the resistance that connects the cathode and an anode. The final step was to select the conductivity and start solving the model. But before start solving the model (step 2: simulation) the element types should be selected. There are three types of elements as per Fig. 4.6.

Constant Element   **Linear Element**   **Quadratic Element**
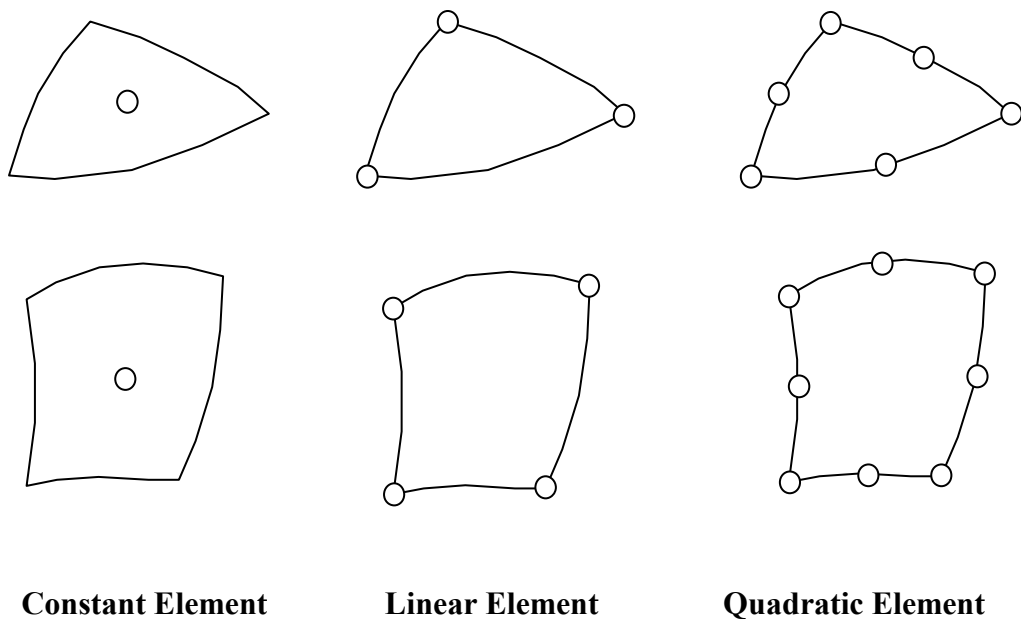
Fig. 4.6 Boundary element types [BEASY, 2009].

The more nodes in the single element the more processing time the software takes. Therefore

the quadratic element will take more simulation time than Linear and constant elements for

the same model. Usually for corrosion and cathodic protection analysis (potential problems)

lower order elements give very satisfactory results.

4.1.2 Two cathodes and single Anode

Defining the geometry

The modeling of this part pursues the same procedure as the first part. The geometry was

built, as in Fig. 4.7. The same model was used for the copper and the HSCI.
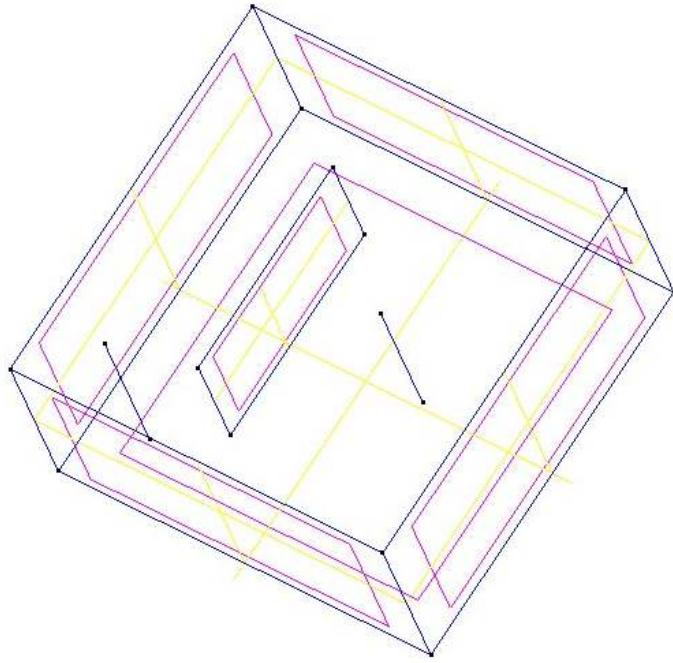
Fig. 4.7 Geometry of two cathodes and single anode model

Mesh Generation

Meshing was generated and separated the geometry into 620 elements, as shown in Fig.4.8.
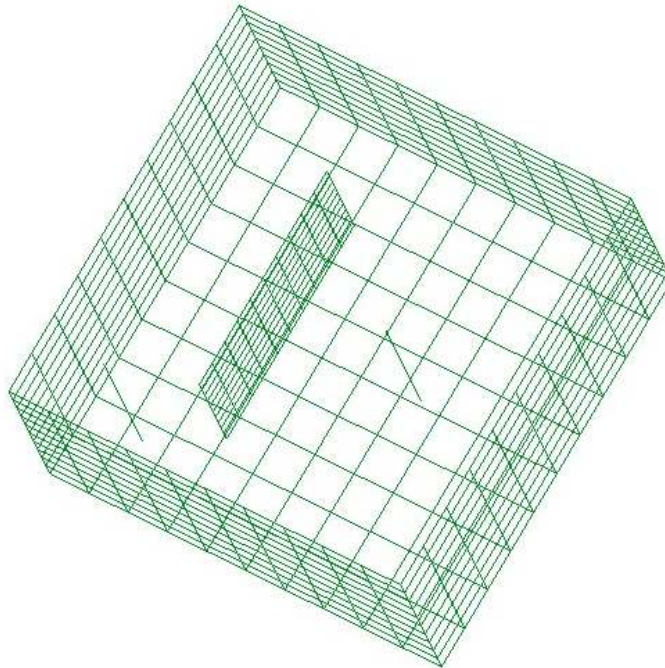
Fig. 4.8 Meshing of the two cathodes and single anode geometry

Boundary conditions

The polarization behavior of both the copper and the HSCI was tested in the same electrolyte, using a potentiodynamic test following the procedure provided in section 3.3 (Fig. 4.9, 4.10). The potential and current density for cathodic side of the curves were numerically input into the BEASY material database, along with the zinc and steel data identified in section 4.1.1. The goal of this step is to solve equation (18) in Chapter 2, Section 2.2.3 which will be used to form the matrix equation (19) in the same section.
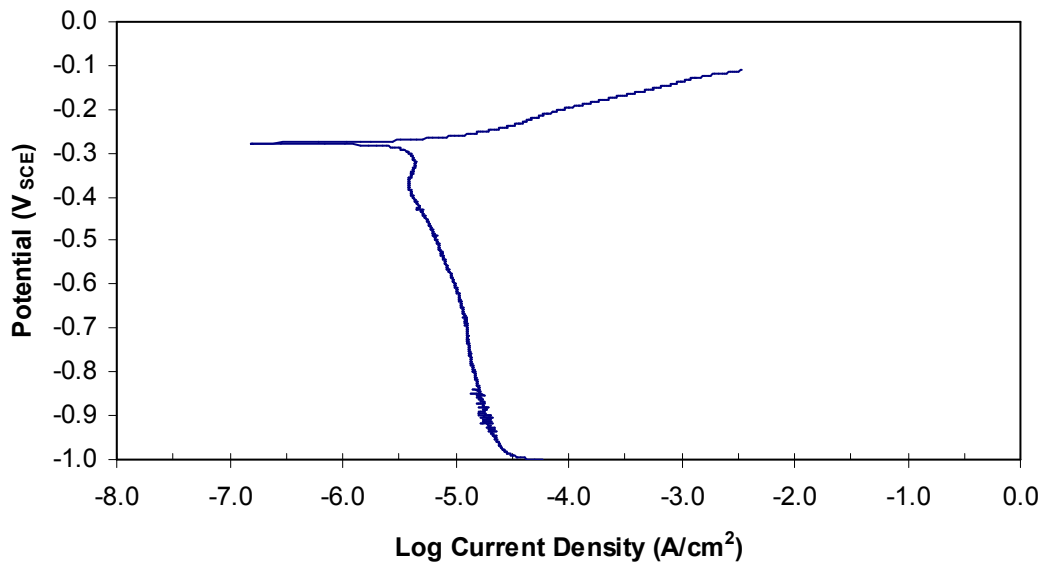

Fig. 4.9 Polarization curve of the copper with 0.1667 mV/sec scan rate and ambient temperature under atmospheric pressure.
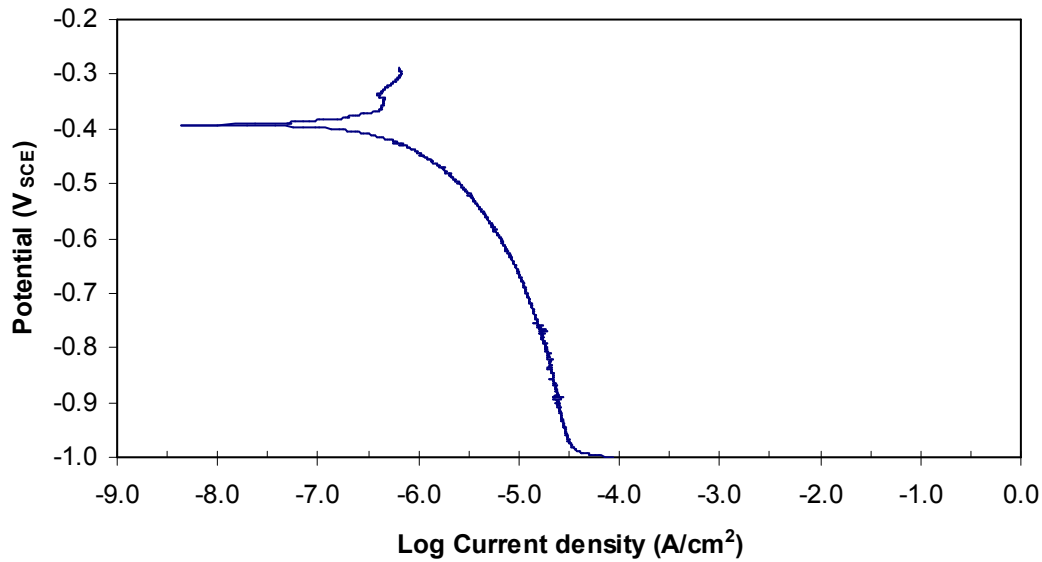
Fig. 4.10 Polarization curve of the HSCI with 0.1667 mV/sec scan rate and ambient temperature under atmospheric pressure.

4.1.3 Application of internal sacrificial cathodic protection

Defining the Geometry

Two sets of magnesium anodes were suspended from the roof. Each set included six anodes. The system was self- controlled, which meant that the cathodic protection will work if the solution covers both the anodes and the tank surface. The tank is typically operated with 20 % load, which ensured that the lower six anodes were immersed in the electrolyte. Fig. 4.11 demonstrates the geometry of the lower portion of the tank. The units chosen for the model were cm, A, and mV, which were compatible with the input data (polarization curves and conductivity).
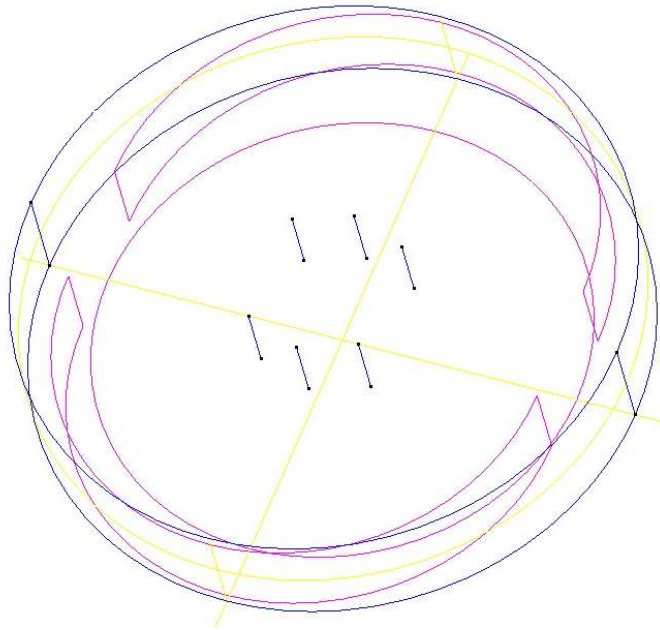
Fig. 4.11 Geometric portrayal of the sacrificial anodes and internal tank cathode

Mesh Generation

The second step was to apply meshing into the geometry of the internal tank surface and on to the anodes as well. The tank and anodes have been separated into 864 elements as show in Fig. 4.12.
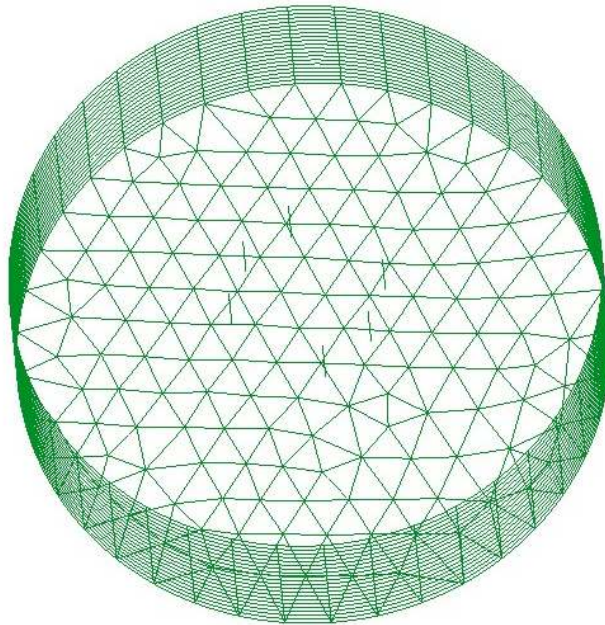
Fig. 4.12 Meshing of the sacrificial anodes and internal tank cathode.

Before the model analysis the polarization of the anodes in the same electrolyte was input into the BEASY software. In the aluminum test, the polarization data of the aluminum was also inputted. The last step was to select the conductivity of the tank, which was 145 mS/cm. These steps reflect that the BEASY CP software was solving and analyzing the problem according to the real conditions of the system.

4.2 Impress current cathodic protection

4.2.1 Simulation of pipe segment

Defining the geometry

The first step in the modeling is to draw the geometry in a GiD program to allow BEASY to read it as in Fig. 4.13
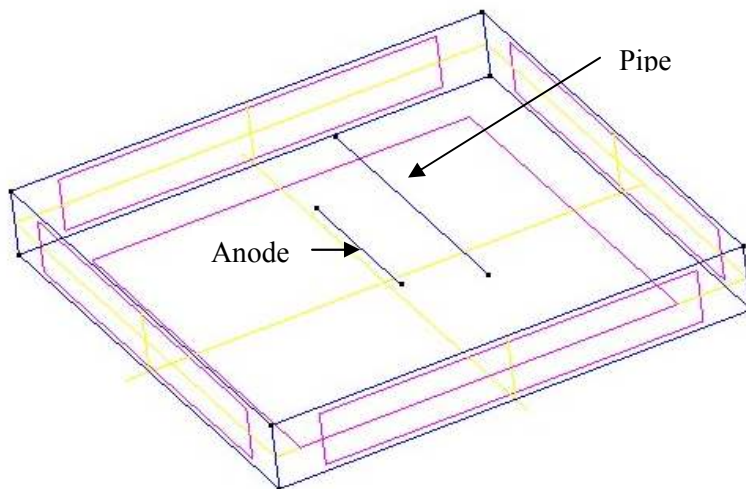
Fig. 4.13 Geometry of the impress current anode and pipe segment

Mesh generation

Once the model is ready, meshes shall be generated to discrete the model into 1145 elements (Fig. 4.14). Then groups have to be identified such as units, anode, polarized material and conductivity.
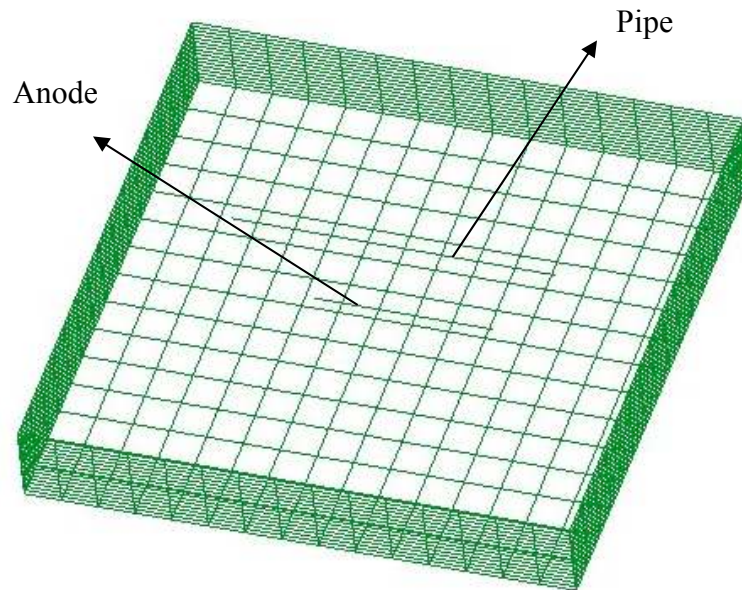
Fig. 4.14 Meshing of the impress current anode and pipe segment

At this point the model is ready to be solved; the file shall be selected and the structures were arranged as electrolyte, cathode and anode by using the BEASY solving tools. In the impress current system the current produced by the anode should be specified which in this case was 1 mA. The material of the cathode was identified as bare steel in the soil; moreover the electrical resistance of the pipeline per length was calculated as follows:

$$R = \frac{\rho}{A}$$

$\rho = 1.18E - 07\Omega m$, resistivity of steel

$A = \frac{\pi}{4}(d^2 - (d - 2t)^2)$ d is the diameter and t is the thickness wall.

$R_P = 2.12E10^{-4}$ Ω/m R_P is the pipe electrical resistance per meter

After the circuit has been set up in the software by choosing the anode, cathode wire

resistance values and power supply (Transformer Rectifier) rating, the next step is to identify

the conductivity of the soil that is calculated as $k = 3.42$ E-3 S/m.

4.2.2 Applications of impress current design

The objective of this section is to review this design by computer modeling to make sure it

provides adequate protection. Fig.4.15 shows the modeling geometry.
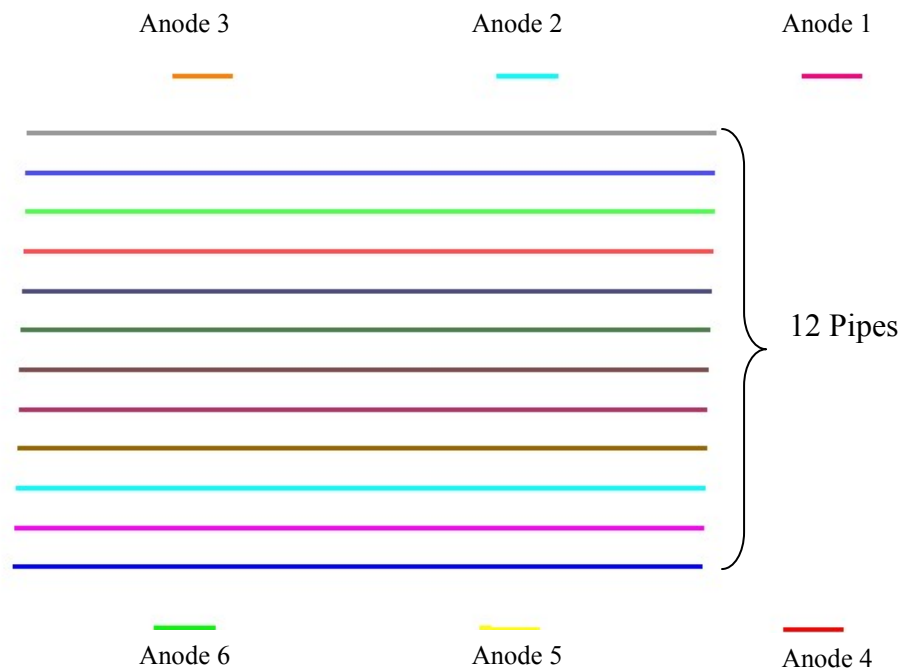
**Fig. 4.15** Geometry for the pipes and anodes of the design.

After building the model, a surrounding box that contains the pipes and anodes has to be drawn to represent the sand soil. As per BEASY guidelines, the size of the soil box should be 20 pipe lengths. Fig.4.16 illustrates the meshing to subdivide the model into 650 elements.
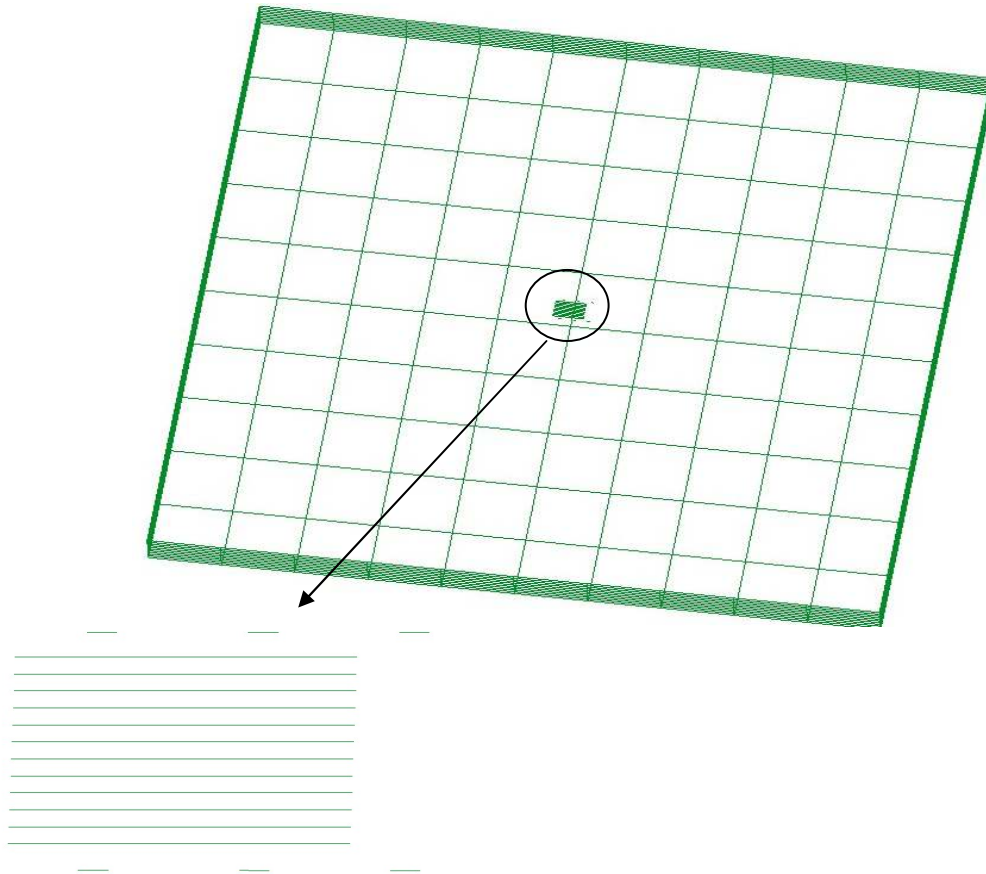

Fig. 4.16 Meshing generation of the pipes, anodes, and the soil box.

Chapter 5

Results and discussion

5.1 Sacrificial cathodic protection

5.1.1 Single cathode and single anode

The experiment had been running for six months, during which period the potential of the plate and the zinc output current were measured every week. The experimental and modeling output were as follows:

1- **Protection potential**

The potential profile in Fig.5.1 showed an approximate 3.8 % error between the experimental and the simulation readings (the first reading of experiment is for the steel natural potential which was measured before the test started). The experimental measurement was taken by the Standard Calomel Reference electrode (SCE).

The profile of the potential on the cathode (steel sheet) is provided in Figure 5.1, using both the experimental and simulation methods. The error margin between the two methods was 3.84%. The source of this error was a voltage drop caused by the instrument, wires, and the reference electrode type. The position of the reference electrode could be another factor in discrepancies in the potential reading.
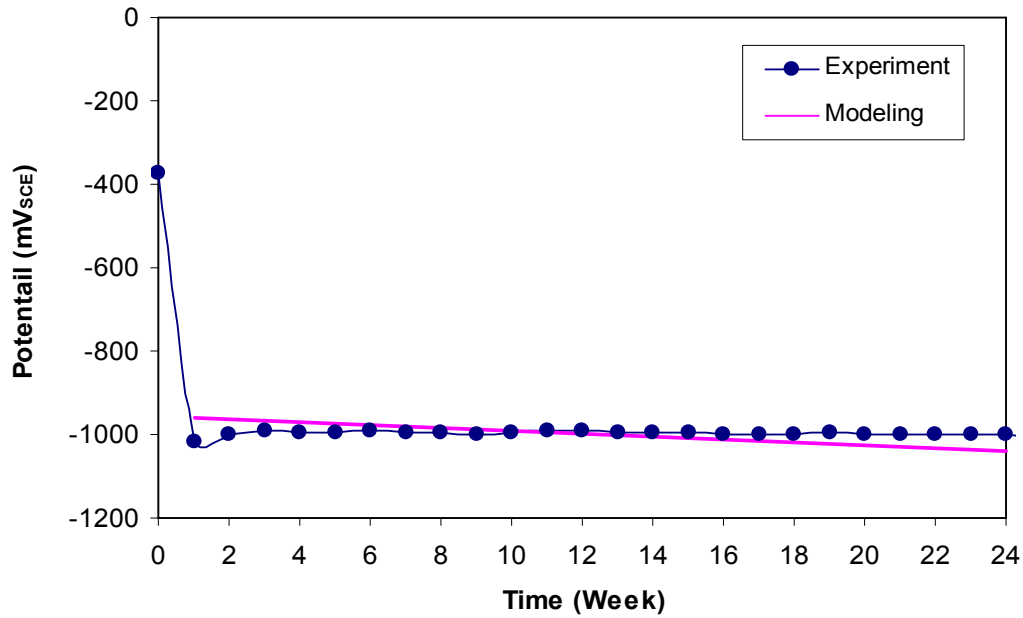
Fig. 5.1 Comparison of experimental and simulation potential readings of the anode.

2- Current

Fig.5.2 illustrates the current profile for both the experimental and simulated results, which started with a 7.9% error between the experimental measurements and the simulation's, which will eventually finish with closer values.

As shown in Fig.5.2, the current profile was plotted for six months. It started with 61 mA, with a fresh solution, and then decayed as the plate polarized to 0.5 mA after 24 weeks. The results in the simulation did not deviate much from this reading, as they started with 66.9 mA and it ended with 0.32 mA in 24 weeks. There was a small deference in the reading because the experiment was working in a very low current scale (mA), and

another error was coming from the instrument and ammeter wire resistance. At the end, this result shows agreement between the experimental and modeling results.
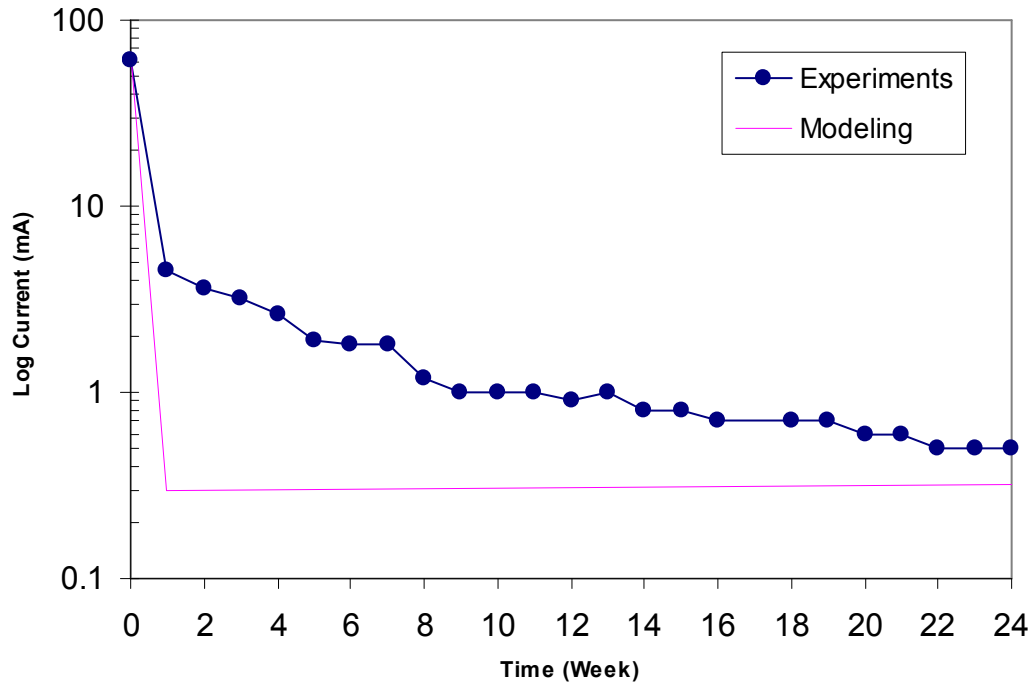
Fig. 5.2 Comparison of experimental and simulation current results of the mild steel sheet.

3- Polarization performance

The polarization performance of the whole system was calculated, using potential against current density which resulted from the output current dividing into the cathode surface area. The calculation of the current density is according to the current divided by the cathode area, so the different current density between the experimental and the simulation results is understandable because it depended on the current obtained, but both approaches show that cathodic protection decreased the current density to an acceptable

level. This would mean a reduced corrosion rate (this is the real objective of the cathodic

protection.)
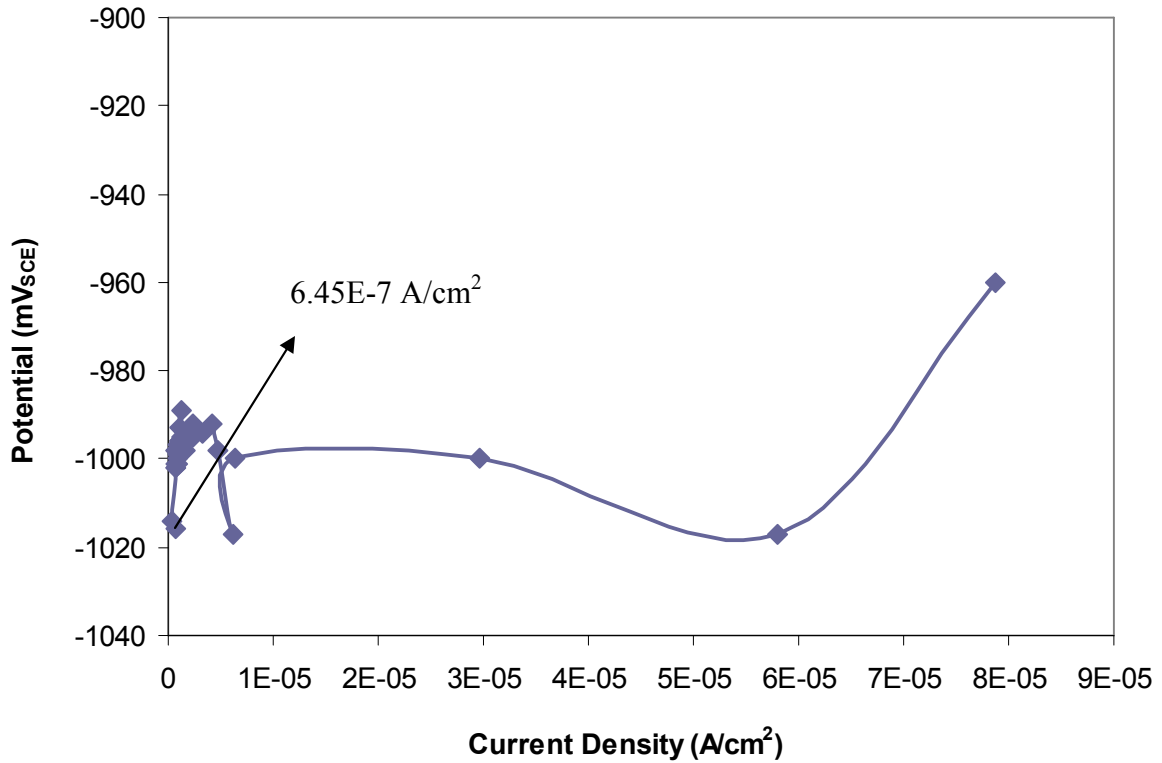
Fig. 5.3 Polarization performance of the mild steel sheet.

Fig.5.3 shows the polarization of the steel sheet using the experimental approach. The final

current density equals 6.45E-7 A/cm^2 while the current density obtained by the modeling was

4.14E-7 A/cm^2. Once the current density is obtained, the corrosion rate can be calculated

using Faraday's law [Jones, 1996]:

$$r_c = \frac{Ia}{nF}$$

Where:

I = Current density.

a = Molecular mass.

F = Faraday constant.

n = number of electrons required for the reactions.

This equation enables the designer of cathodic protection system to calculate the anodes lifespan ahead before start the installation. This valuable information output validates that BEASY software is a powerful tool in the application of cathodic protection.   On the other hand, Fig.5.4 gives a visual demonstration of the potential distributions for the entire system.
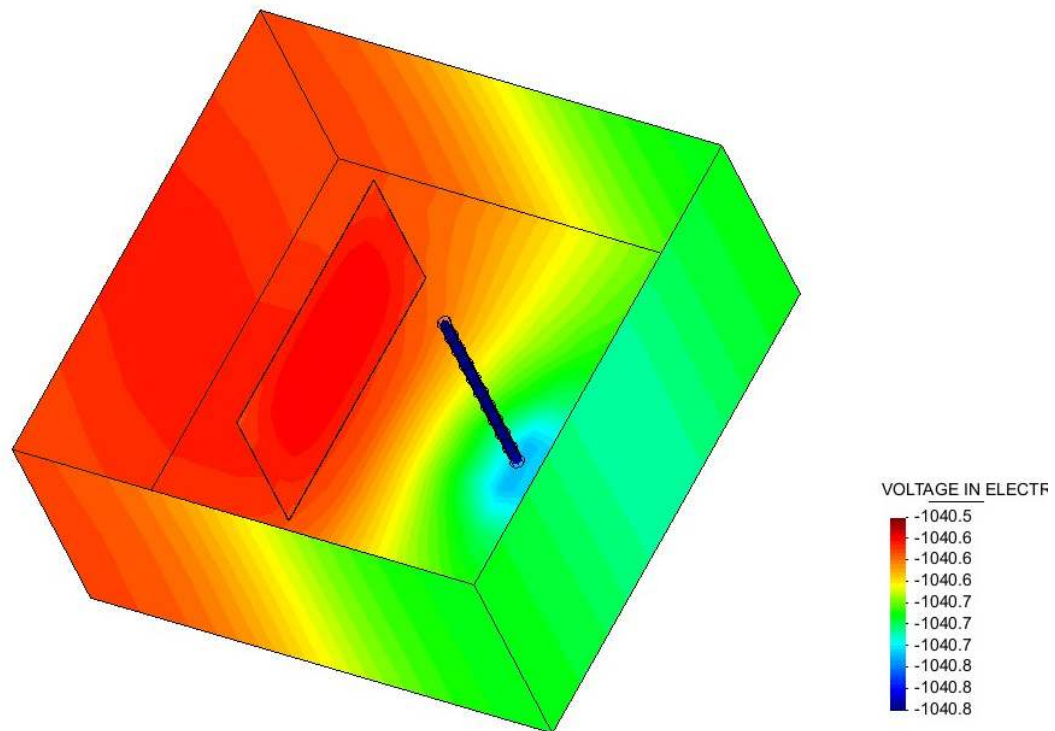
Fig. 5.4 Potential distribution for the single cathode single anode (mV_{SCE}).

Finally, the most important factor that is needed to evaluate the efficiency of the cathodic protection system is the potential of the carbon steel. As per Fig. 5.4 the lowest potential in the carbon steel plate is -1040.5 mV. This potential is more than what NACE specifies in the criteria of cathodic protection potential which is -850 mV [NACE, 2004]. The potential result was used by previous studies to evaluate the accuracy of the modeling technique. Brichau found the maximum error in the potential between the simulated and measured result is 15% [Brichau, 1994] while Zamani found that the difference is 6% between the actual and the computed potential [Zamani, 1988].

On the other hand DeGiorgi used the current measurements to evaluate the different shapes of the propeller as mentioned in Chapter 2 section 2-3 [DeGiorgi, 2005].

5.1.2 Two cathodes and single anode

The current flow between the zinc anode and the cathode (steel and copper or steel and HSCI) was recorded for 24 hours as in Table 5.1 and Figure 5.8.

Table 5.1 Experimental current drainage output values.

Time (hours)	current of Fe (mA)	current of Fe & HSCI (mA)	current of Fe & Cu (mA)
0	61	115	125
0.1666	29	47	76
0.25	23	40.2	67
0.5	18.5	26.7	53.4
1	12.2	15.6	39.8
2	7.4	8.9	23.5
3	6.2	7.9	15.6
4	5.5	7.6	12.2
5	5	7.4	11.3
6	4.9	7.2	11.1
24	4	6.6	9
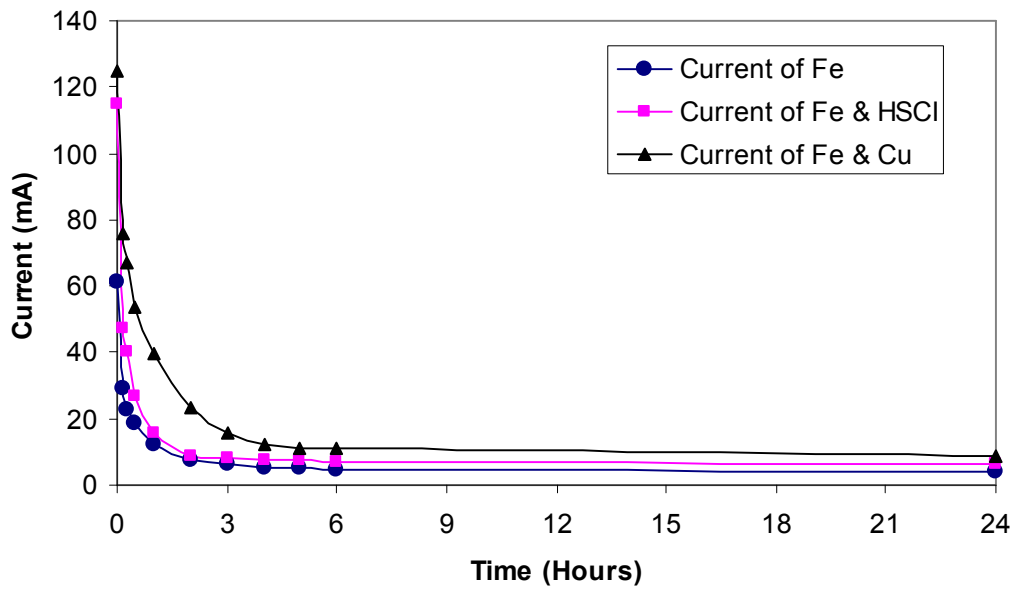
Fig. 5.8 Current drainage curve of the materials.

Simulation Results

The net current for the model after polarization was:

Table 5.2 Simulation output values for current drainage.

Materials	current of Fe & HSCI (mA)	current of Fe & Cu (mA)
Current Value	7.02	9.7

Discussion

The results of the experiment and the simulation demonstrated the current drainage of the

zinc anode, when it is connected to the different materials either steel with copper or steel

with HSCI. On the experimental side, the final current running through the steel and HSCI

was 6.6 mA, while it was 7.02 mA in the simulation, which produces a 6.4% error. On the

other hand, in the experiment, the current jumped to 9 mA when the zinc anode connected to

the steel and copper rod, while the final current was equal to 9.7 mA in the simulation, with a

7.7% error. The fact that the experiment and simulation give approximately the same current

values reflects the accuracy of the BEASY simulation software. Although the HSCI rod had

a higher surface area, the current drainage was reduced by 37% when it was replaced copper

rod. Metwally et al. reduced the current drainage by approximately 50% by replacing the

copper earthling rod by aluminum [Metwally, 2008].

The soundness of BEASY software is once again confirmed for the following reasons:

1- The experimental result closely matches the output of BEASY software.

2- The result of this experiment is consistent with the output of BEASY software
because copper is seeking more current.

5.1.3 Application of internal cathodic protection

In this section both magnesium and aluminum alloy were tested and the experimental results

are as follows:

 Magnesium

The magnesium anode was examined using electrochemical techniques (Fig. 5.9, 5.10). The

open circuit potential started around -1.9 V_{SCE} and reached quasi steady state at -1.7 V_{SCE}. In

Fig. 5.10 magnesium corroded at a very low current density (approximately 1E-5 A/cm^2).

The magnesium started to passivate at -1.12V_{SCE}, which is the protective potential window of

carbon steel. The Scanning Electron Microscopy (SEM) morphology of the magnesium after

the test showed a passive layer on the surface with some localized pitting dispersed (Fig.

5.11). The Energy-Dispersive X-ray Spectroscopy (EDX) analysis in Fig.5.12 for the

corrosion surface showed high magnesium (75%) and oxygen (23%) contents. This could be

an indication of the formation of MgO and/or Mg(OH)$_2$ as already discussed by Pinto et. al. [Pinto, 2010].
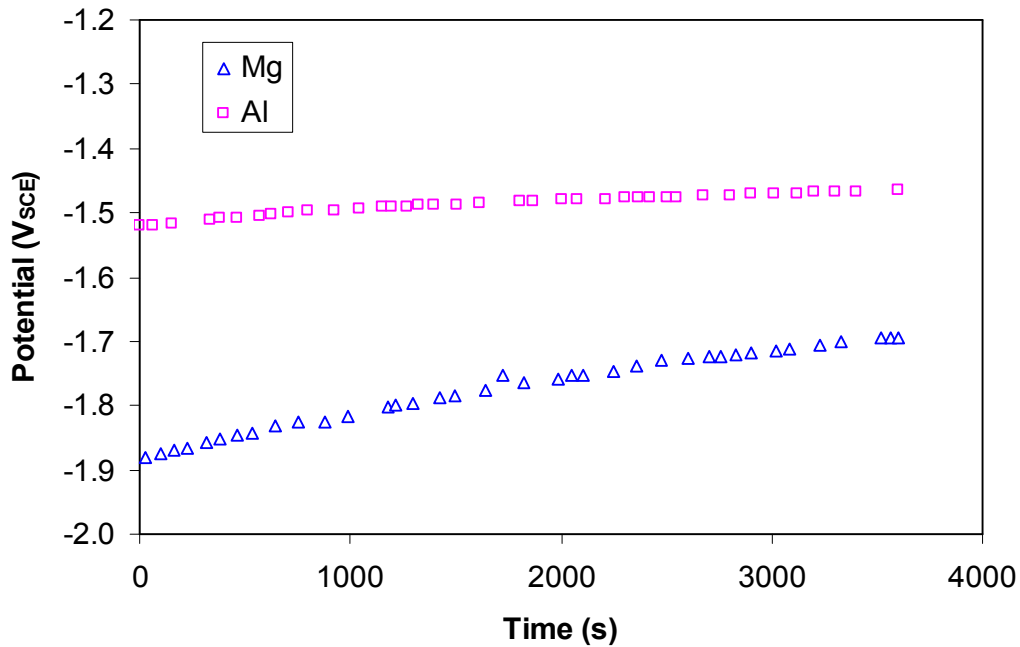
Fig. 5.9 Open Circuit Potential for magnesium and aluminum alloy, 60 ^{0}C in the tank electrolyte (Table 3-4).
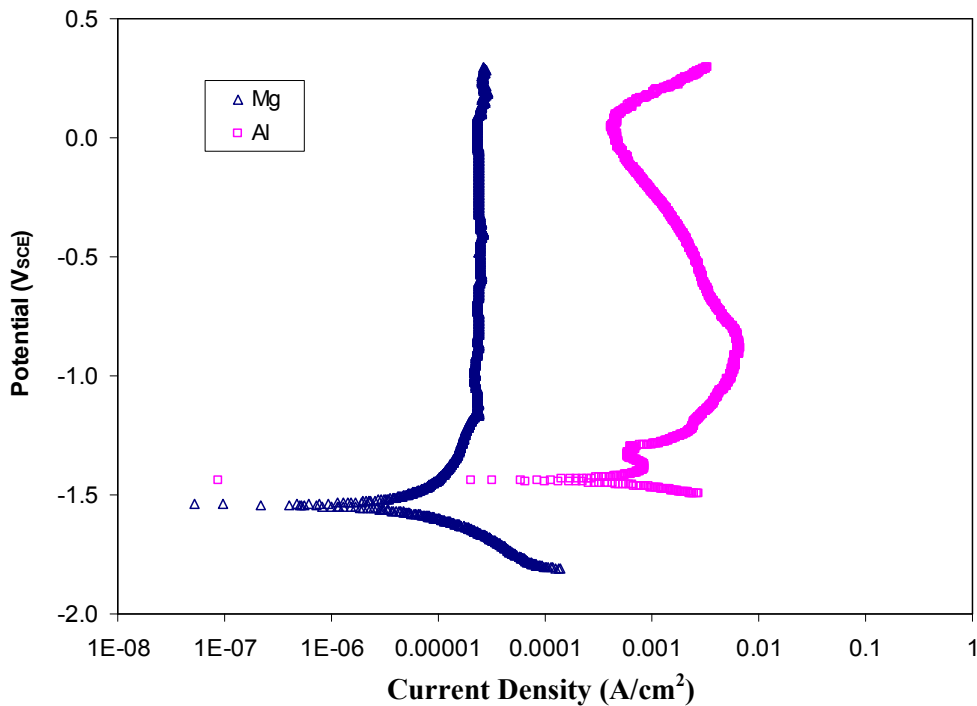
Fig. 5.10 Potentiodynamic Polarization curve for magnesium and aluminum alloy anodes, 60 ^{0}C in the tank electrolyte (Table 3-4).
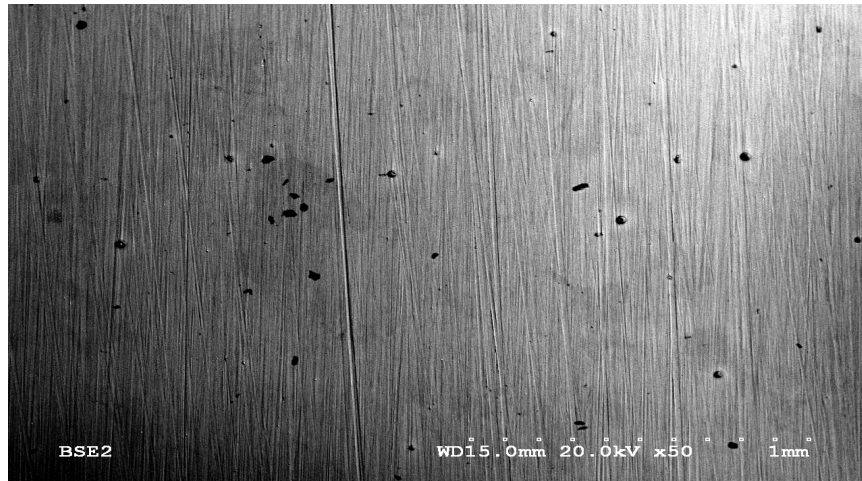
Fig. 5.11 SEM morphology for the magnesium surface layer after the test.
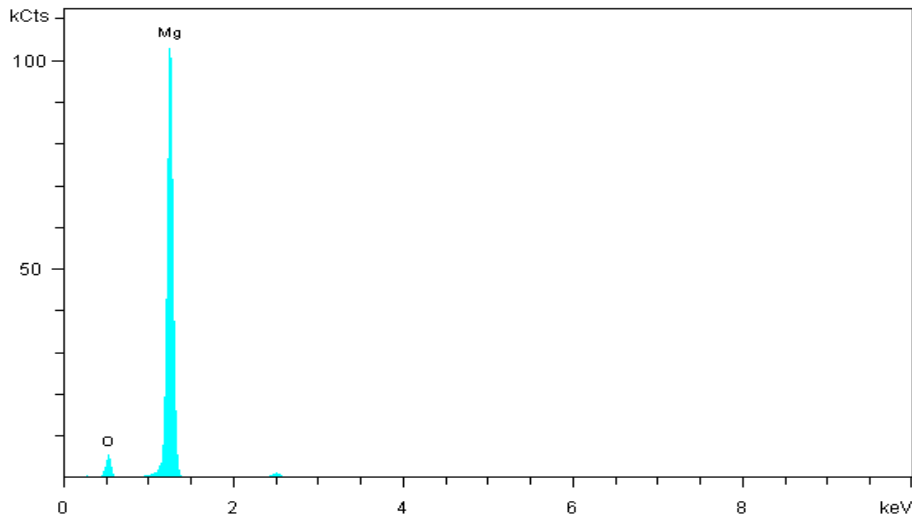
Fig. 5.12 EDX analysis for the magnesium surface layer.

The E-pH (Pourbaix) diagram for the magnesium-water at 60 ^{0}C Fig.5.13 was generated by HSC Chemistry program version 5.11. E-pH diagram shows that the major species exist are magnesium ions Mg^{2+}, until the solution reaches pH value of 7.4, where $Mg(OH)_2$ precipitates as reported by previous studies [Perrault, 1974],[Badawy, 2010]. Moreover, the efficiency of magnesium when it's used as sacrificial anode is 50 % [Genesca1996].
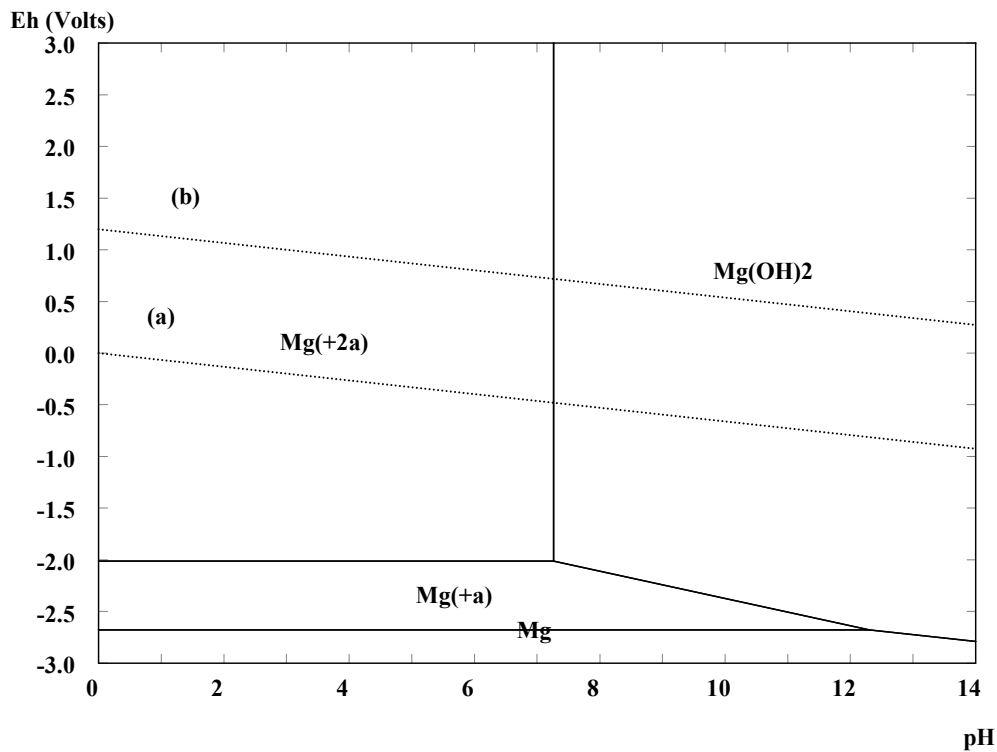
Fig. 5.13 E-pH (Pourbaix) diagram for the magnesium-water system at 60 ^{0}C, (a) and (b) lines are H_2O limits.

Therefore, the magnesium anode was not a proper choice for protecting the carbon steel in this environment.

Aluminum

Since pure aluminum cannot be used as anode in cathodic protection because it will be passivating, an aluminum alloy was used [Baeckmann, 1997]. The open circuit potential (OCP) for the aluminum alloy is about -1.5 V_{SCE} (Fig. 5.9). During the potentiodynamic polarization test, the aluminum alloy produced a high current density (0.7 mA/cm2), as illustrated in Fig. 5.10. The behavior of the anode showed an active region for potentials between -1.4 V_{SCE} to -0.75 V_{SCE} with a high current density. This is the potential protective window for carbon steel.

73

Modeling results

Figure 5.14 shows the potential distribution of the tank's internal wall protected by magnesium anodes. The potential level was very low and almost equal to the natural potential of the carbon steel (-440 mV). Moreover, the current produced by the anodes was less than 1 A, and the current could not polarize the carbon steel cathode. On the other hand, the potential on the same structure (internal wall of the tank) rises by replacing the material of the anodes with aluminum alloy (Fig.5.15). The lowest potential was around -700 mV$_{SCE}$ and it reached -850 mV$_{SCE}$ in some areas. The current produced by the aluminum alloy anode was high. It reached 37A in total which is enough to polarize all parts of the tank. According to NACE standard RP0196 [NACE, 2004], section 6, the potential protective criteria was -850 mV between the cathode surface and the copper/copper sulfate (Cu/CuSO$_4$) reference electrode—or a minimum of 100 mV of cathodic polarization. These criteria were achieved, as shown in Fig. 15, by using aluminum alloy anodes.

POTENTIAL (Average
-495.44
-495.78
-496.12
-496.46
-496.8
-497.14
-497.48
-497.82
-498.16
-498.5
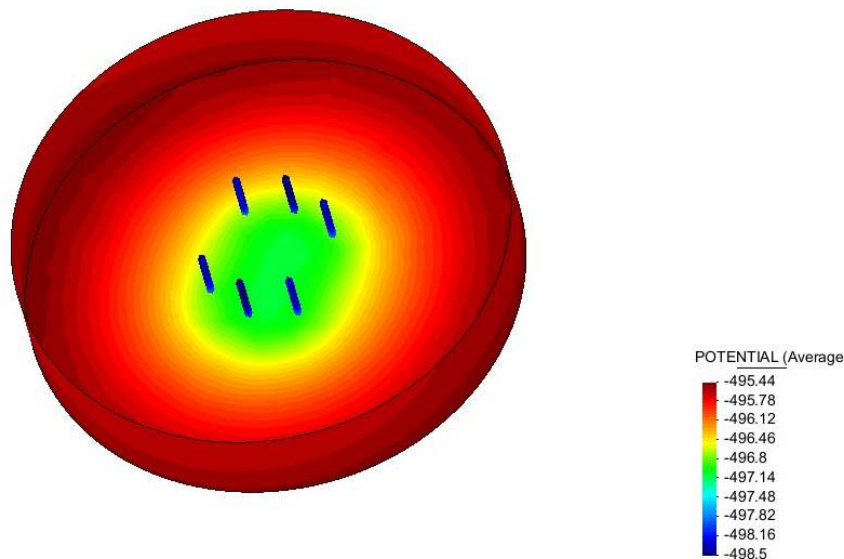
Fig. 5.14 Potential distribution in the tank with magnesium anodes (mV$_{SCE}$).
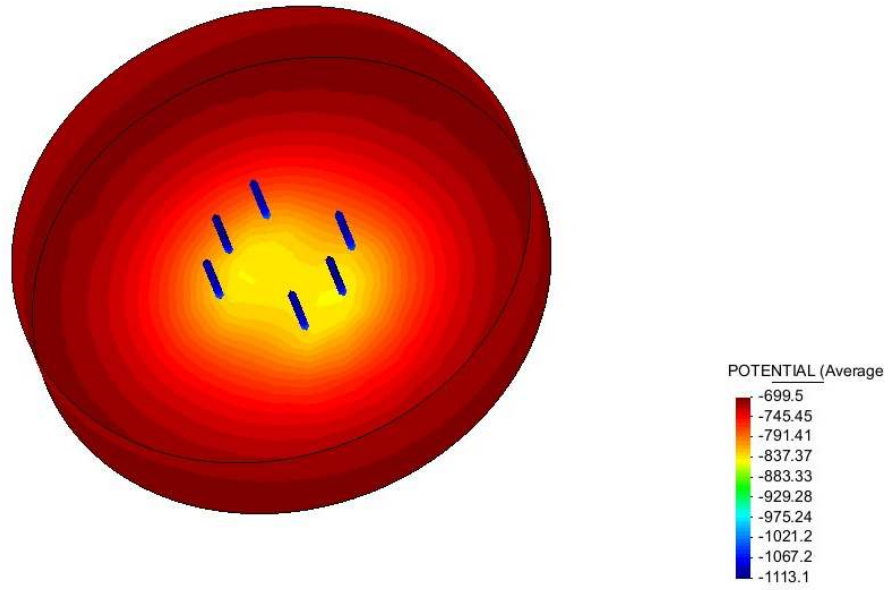
Fig. 5.15 Potential distribution in the tank with aluminum anodes (mV_{SCE}).

Regarding previously mentioned issues associated with modeling of cathodic protection, interference, location of anodes and coating, in this application, the stray current interference cannot occur because the tank is fully isolated in this closed system. Moreover, the possibility for the optimum control of the anodes in this application is done already by suspending the anodes from the roof. The internal tank wall is bare steel and so there was no influence of coating.

5.2 Impress current cathodic protection

5.2.1 Simulation of pipe segment

Experimental results

The natural potential of the pipeline was taken before connection at eight points between the surface and $Cu/CuSO_4$ reference electrode and the average was $E = -300 \ mV_{Cu/CuSO4}$

| -298 | -321 | -301 | -295 | -303 | -288 | -300 | -285 |
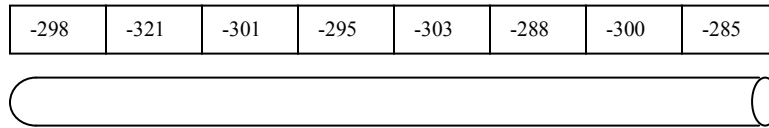
Fig. 5.16 Natural potential of the pipe segment ($mV_{Cu/CuSO4}$)

By means of connecting the circuit to the power supply the anode was setting to discharge 1 mA DC current. The instant off (off potential) of the pipeline was measured by switching off the power supply and taking the reading immediately in approximately one second. The potential in the cathode surface once it's polarized was E_{off} = - 630 $mV_{Cu/CuSO4}$ as in Fig. 5.16.

Simulation result

 The simulation result demonstrates potential varying from -605 $mV_{Cu/CuSO4}$ to − 618 $mV_{Cu/CuSO4}$ as shown in Fig.5.17.

POTENTIAL on tubes
-605.71
-607.14
-608.57
-610
-611.42
-612.85
-614.28
-615.71
-617.13
-618.56
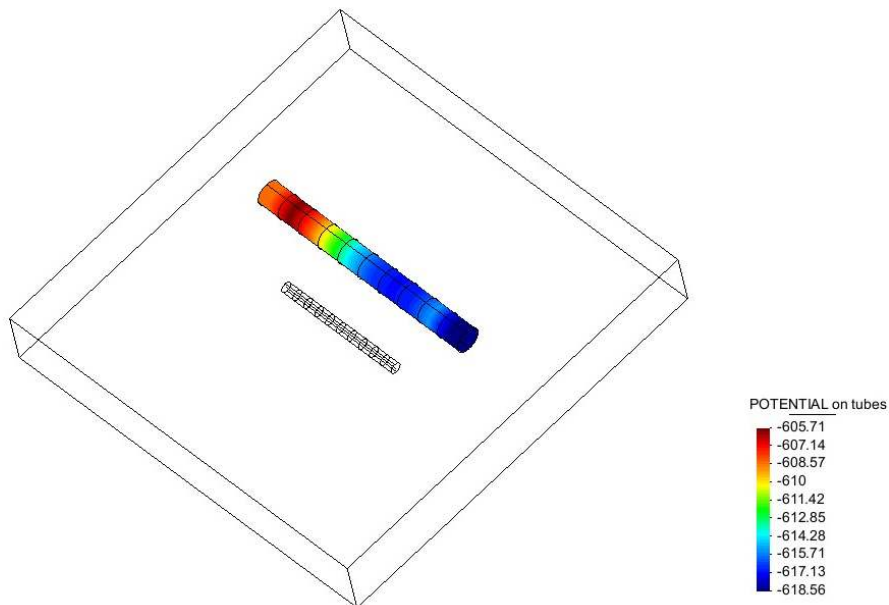
Fig. 5.17 Potential distribution on the cathode ($mV_{Cu/CuSO4}$)

76
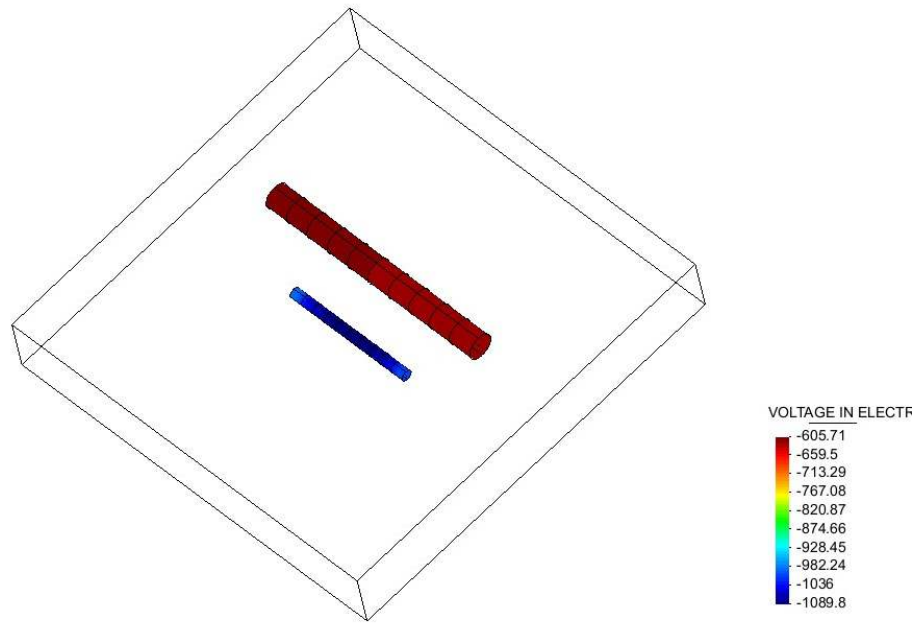
Fig. 5.18 Potential of the pipe and anode (mV$_{Cu/CuSO4}$)
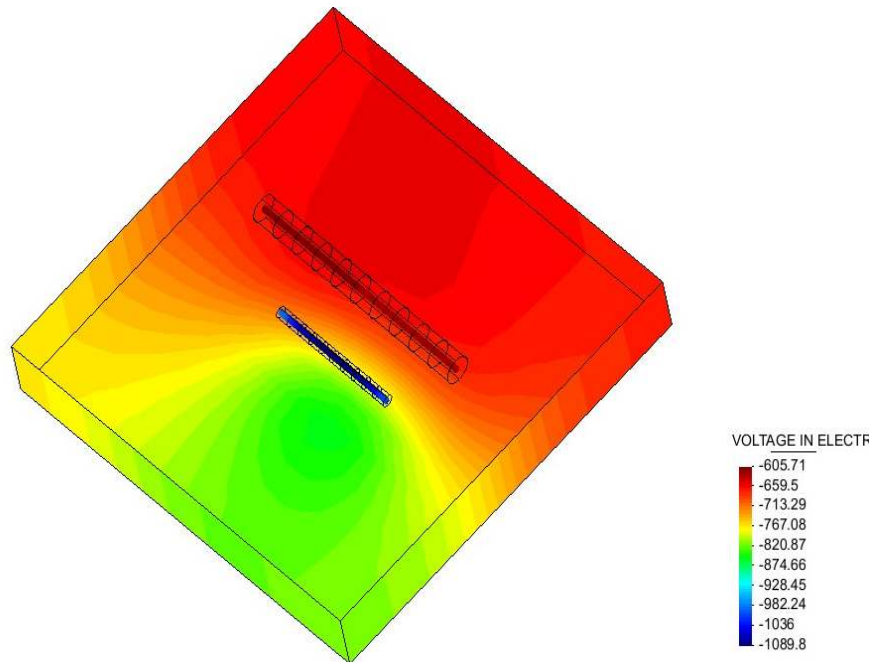
Fig. 5.19 Potential distribution on the whole system (mV$_{Cu/CuSO4}$)

Discussion

Once the pipe and anode were connected to the power supply, the cathode starts polarizing but this polarization is limited by the high resistivity of the soil. Therefore, the anode could

not feed more current, and the maximum current discharged was 1 mA. The off potential of the cathode reached -630 mV $_{Cu/CuSO4}$. The off potential had eliminated the IR drop to get accurate results [Zakowski, 1999] [Qiu, 2004].

The best cathodic protection criterion in the case of high resistivity is to apply 100 mV$_{Cu/CuSO4}$ shifts from the natural potential. The system satisfied this criterion as there was more than 300 mV$_{Cu/CuSO4}$ shift. Figures 5.18 and 5.19 show the reading computed by the BEASY software which is -611 mV$_{Cu/CuSO4}$ with 3% error compared to the actual reading, and since the software calculated the potential on the surface of the structure, there was no need to consider the IR drop. A similar work was reported in the computer simulation of cathodic protection for a section of pipeline [Kasatkin, 2003] with maximum error of 9%. The result obtained from the software provides more details to interpolate and evaluate the cathodic protection system. The voltage gradient between the anode and the cathode is a decent tool that helps understand the effect of soil resistivity as illustrated in the curve below (Fig.5.20) showing potential distribution vs. the 15 cm distance between the cathode and the anode.
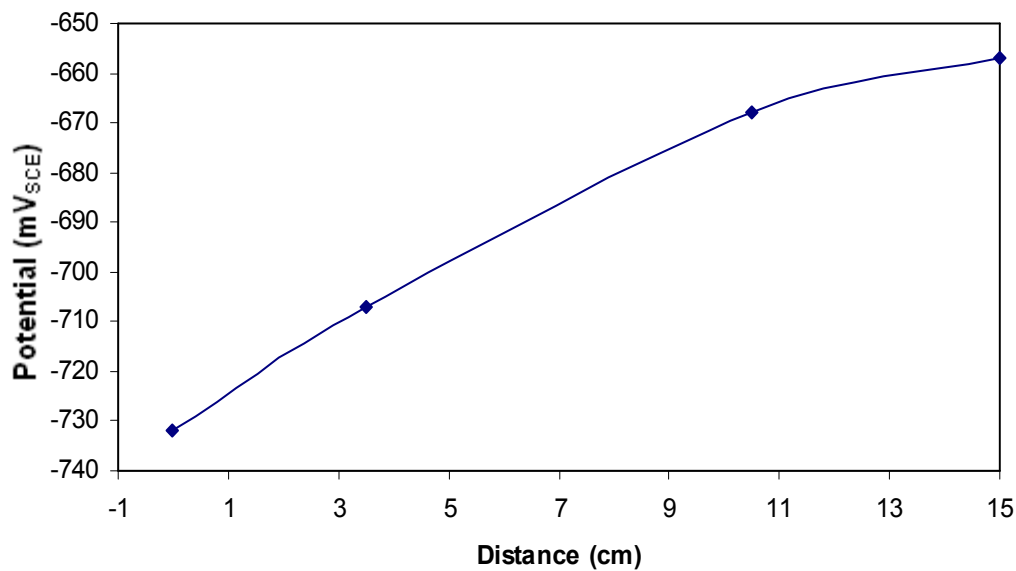
Fig. 5.20 Voltage gradient vs. distance between cathode and anode.

5.2.2 Application of impress current design

A real industrial design was modeled using the BEASY CP software. The system contained six anodes. The model was solved in several stages. In the first stage, each anode is configured to discharge 1 Amp as in Fig.5.21. The current of the anodes will be increased gradually until enough protection is provided.
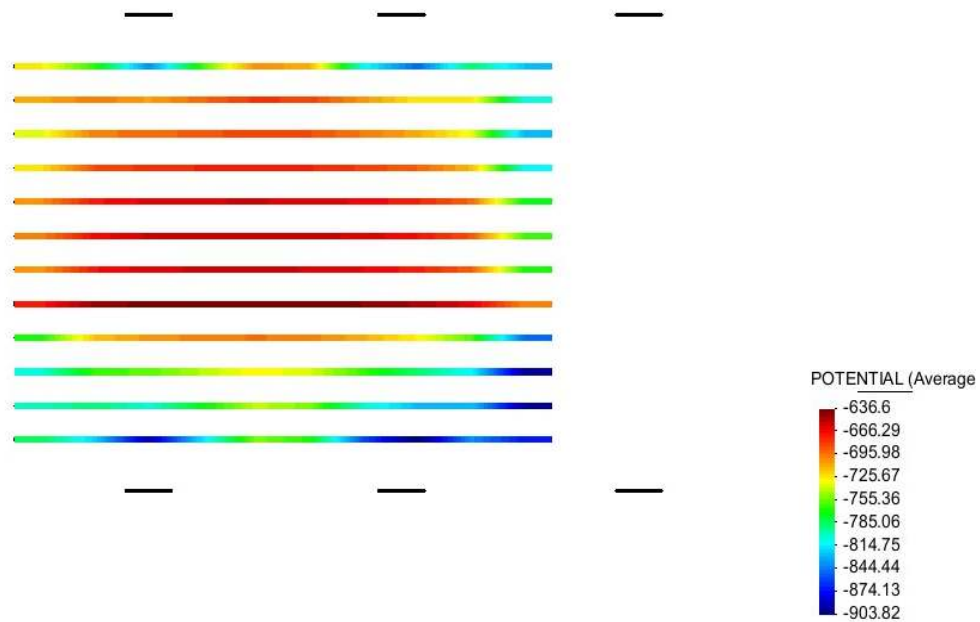
Fig. 5.21 Average potential (mV$_{Cu/CuSO4}$) of the pipelines with 1 Amp.

The above figure illustrates that there are low protection areas with potential -636.6 mV $_{Cu/CuSO4}$. The maximum potential is -903.82 mV$_{Cu/CuSO4}$.

The next stage is to increase the current discharge by each anode up to 2 Amp as in Fig.5.22.
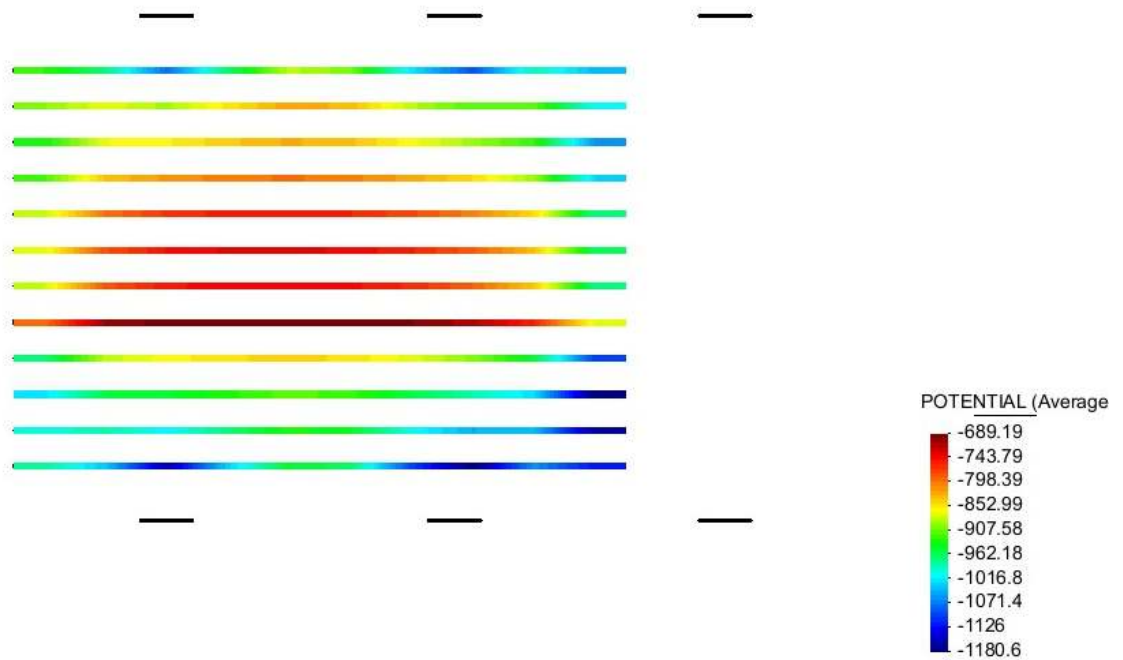
Fig. 5.22 Average potential distribution (mV$_{Cu/CuSO4}$) on the pipeline using 2 Amp.

Fig. 5.22 shows that the protection level has been increased but still there are certain areas in the middle that do not receive enough protections. The maximum potential now is -1180 mV $_{Cu/CuSO4}$ which appears in the closest points to the lower row of anodes. Therefore, the upper row of anodes shall be increased up to 3 Amp. per anode and the lower anodes keep the current level.
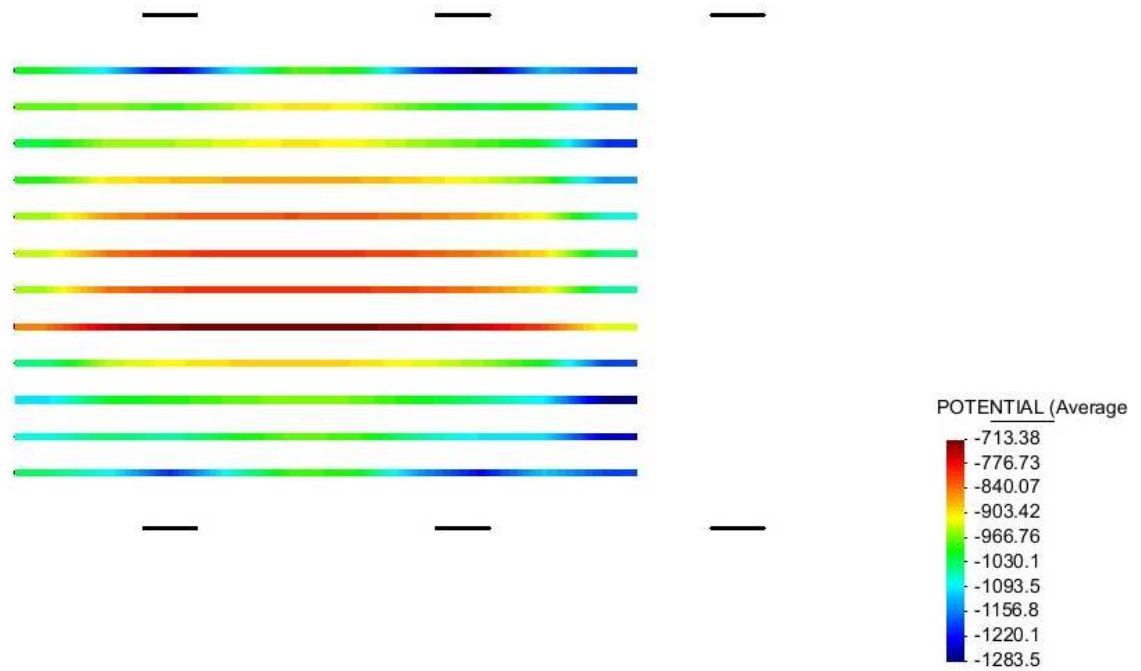
Fig. 5.23 Average potential distribution (mV$_{Cu/CuSO4}$) of the pipelines in third stage.

The potential in the third stage is improving by carefully distributing the current on the

anodes as in Fig. 5.23. The lowest potential is -713.38 mV $_{Cu/CuSO4}$ which it accepted as per

NACE standard because it is more than the natural potential by -200 mV$_{Cu/CuSO4}$. The total

current for the anodes is 15 Amp and that is more than what the designer considered for the

transformer rectifier rate (12 A). The third pipeline from the top receives more potential

(more blue color) than the second one because it's smaller in its diameter. Fig.5.24 shows

the actual potential distribution on the pipelines from when zoomed in.
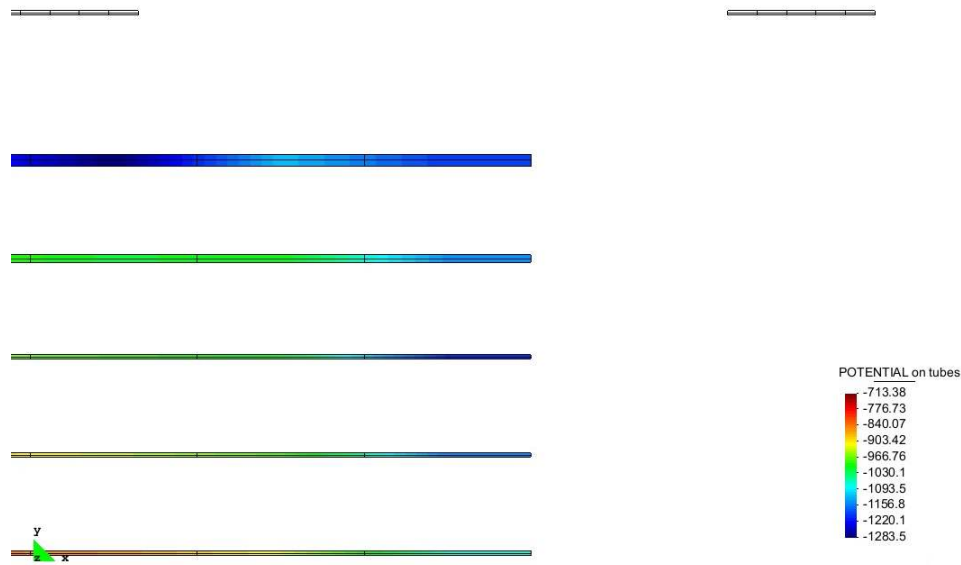
Fig. 5.24 Actual potential distribution on the pipes (mV$_{Cu/CuSO4}$).

As Orazem et. al. modeled the cathodic protection of an existing pipeline with sacrificial anodes, the computer simulation is useful in cathodic protection design [Orazem, 1997]. They increased the number of sacrificial anodes (to feed more current) until the potential exceeded -850 mV$_{Cu/CuSO4}$. Lacerda et. al. [lacerda, 2007] also modeled an experiment of cathodic protection for a steel pipe with both one and two anodes. Their experimental and modeling results demonstrate that the potential increases with growing number of anodes. In our simulation, however, the current of the anodes increased gradually in order to achieve better protection. Similar studies were discussed in section 2-4-2, which showed optimum locations of anodes and reference electrodes.

But the design was for coating pipelines with 15% defect in the coating. The presence of the coating on the surface of the pipeline will decrease the required current density. Therefore the polarization curve of the bare pipeline will be shifted toward lower current density. The following figure represents the potential distribution of the coated pipelines with 1 ampere discharged from each anode.
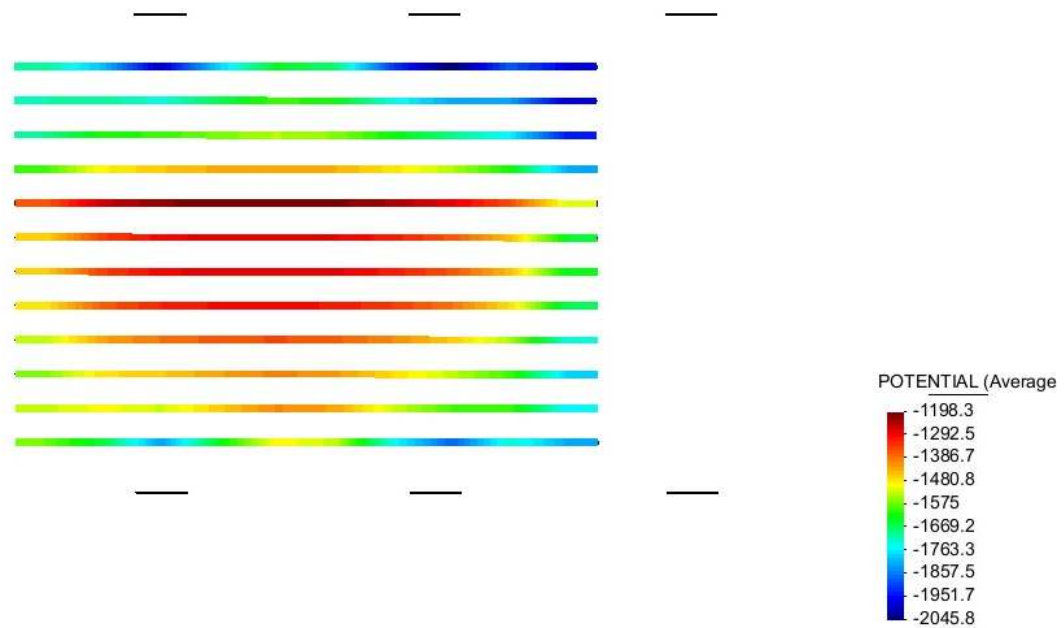
Fig. 5.25 Potential distribution ($mV_{Cu/CuSO4}$) on the coating pipelines with 1A.

Fig.5.25 showed high potential on the pipelines. The minimum potential is -1198.3 $mV_{Cu/CuSO4}$ and the maximum potential is – 2045.8 $mV_{Cu/CuSO4}$ which is a high potential and poses dangers on the coating and perhaps will lead to hydrogen embitterment and localized corrosion later on. The best solution is to lower the supplied current to 0.5 A per anode in order to reduce the effect of over-potential.
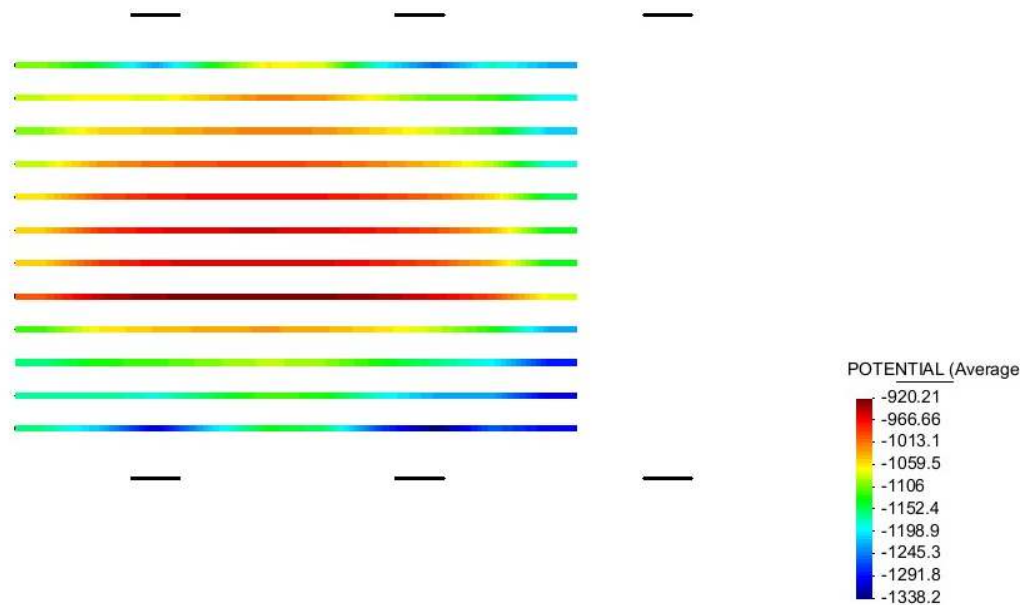
Fig. 5.26 Potential distribution (mV$_{Cu/CuSO4}$) on the coating pipelines with 0.5 A.

Fig. 5.26 reveals that by reducing the supplied current, the potential dropped down. The lowest potential is now -920.21 mV$_{Cu/CuSO4}$ which is more than the NACE standard potential criteria (-850 mV) while most of pipelines have potential less than -1200 mV$_{Cu/CuSO4}$. The potential that occurs on the nearest point from the anode is still too high -1338.2 mV$_{Cu/CuSO4}$ and this can be avoided by moving the anode away from the pipelines.

This application indicates that BEASY software can be used effectively to simulate the cathodic protection of bare and coated structures. Moreover the validation of the cathodic protection design can be done before installation. The BEASY software can be used as a learning tool to show the effect of coating on the cathodic protection system.

The modeling of cathodic protection associated with coating was studied and validated previously in chapter 2 section 2-3-3. Degerstedt et. al. use the computer simulation to model

a 30.48m long pipeline segment with 85% coating effectiveness. [Degerstedt , 1996] Their

study incorporates three cases to represent 15% defect in coating. All cases involve

extremely small amounts of current flowing in the circuit due to the influence of coating.

DeGiorgi and Hamilton also validate perfect coating assumptions in their computer modeling

of cathodic protection [DeGiorgi, 1995].

Chapter 6

Summary and conclusion

Cathodic protection is an electrochemical technique to control corrosion. The design of cathodic protection system relies on the experience, skills of the cathodic protection engineer and appropriate mathematical formula. However, when an installation of the cathodic protection system is completed, corrections or adjustments on the system will be costly. The simulation enables the engineers to predict and test a cathodic protection system prior to installation to prevent further costs. There are three numerical methods employed to simulate the cathodic protection: Finite Deferent Method, Finite Element Method and Boundary Element Method. BEM offers advantages as cathodic protection parameters include the potential and the current density which are calculated on the boundary of the surface. The boundary element based BEASY software was used in this study to confirm the experimental output so that the software can be used in industrial applications. The study was conducted on the sacrificial and impresses cathodic protection.

In the sacrificial cathodic protection, two experiments were conducted to test and learn the capabilities of BEASY software. First, pure zinc was used to protect mild steel. The experiment had run for six months to give the cathodic protection system enough time for stabilizing. The experimental and simulation results match closely in three parameters namely: potential, current and current density. In the second experiment, the current drainage was observed on two cathodes (mild steel with HSCI or copper) connected to the zinc anode. The results showed that the current drainage of the copper was higher. The simulation computed the current drainage of each metal with maximum 7.7% error. As a part of the

simulation requirement, the potentiodynamic curve of zinc, mild steel, copper and HSCI were generated.

In the application of the sacrificial cathodic protection, the BEASY software was used to investigate the failure of magnesium anode in the storage tank containing alkaline solution. The possibility to use aluminum alloy as an anode instead of magnesium was studied. The magnesium anode was tested in both high pH and high conductivity solutions, and showed passive behavior. The dominant species of the magnesium was the $Mg(OH)_2$, as confirmed by the E-pH diagram. Moreover, the simulation results demonstrate that the magnesium anode cannot feed enough current to polarize the inside of the carbon steel tank. In contrast, the aluminum alloy anode gives a current density high enough to push the carbon steel potential to less than -700 mV.

Therefore, it is concluded that the aluminum alloy anode is more suitable for high pH and high conductivity media. It gives a higher current rate and higher potential, as shown in the simulation results. The BEASY software proved to be a useful tool in the simulation of the cathodic protection system.

The experiment of impress current cathodic protection of a small pipeline segment protected with high silicon cast iron in a sand soil was conducted. The BEASY CP software results matched experimental measurements. The error in the potential of the cathode was only 3%. The BEASY CP software provides more information that helps the user evaluate a CP system. One of the most helpful tools in simulation of the impress current CP system in the soil is the voltage gradient that was difficult to predict. The high resistivity soil worked as a barrier for the current to move from the anode to the cathode.

Subsequently, a real cathodic protection design for 12 pipelines protected with six anodes was simulated in two cases. In the first case, the pipeline surface was bare. The results demonstrated that high current was required to polarize the pipelines. The BEASY gave the user more options to change the anode current output to reach the optimum protection. The second case was for the same pipelines with 15% coated defect on the surface. In this case, lower current requirement caused over-potential on the surface which had some consequences such as hydrogen embitterment. The BEASY software was a powerful tool to assess the design: to verify the anode location and over-potential. Moreover, BEASY can be used as a learning tool for new engineers to show the influence of coating on the cathodic protection.

Recommendations for future work

- A pipe with a variety of coating is recommended to be tested experimentally and simulated to calculate the accurate breakdown factor that should be used in the future to represent the coating conditions.

- Anodic protection is widely used in the industry to protect the plant facilities e.g. tanks and heat exchangers that are exposed to an acidic environment such as sulfuric acid (H_2SO_4) and phosphoric acid (H_3PO_4). Anodic protection is achieved by raising the potential to the passive region of the materials. It is recommended to simulate the process of anodic protection to validate feasibility.

References

Abootalebi.O, Kermanpure, A, Shishesaz M.R. and Golozar M.A. 2010. Optimizing the electrode position in sacrificial anode cathodic protection systems using boundary element method. Corrosion Science 52-678-687.

Adey, Robert A. and Baynham, John. 2000 A. Computer simulation as an aid to the CP system design and interference prediction. Paper presented in CEOCOR 2000 conference. Brussels, Belgium.

Adey, Robert A. and Baynham, John. 2000 B. Design and Optimisation of cathodic protection system using computer simulation. Corrosion/2000, paper no.723 (Orlando, Florida: NACE 2000).

Adey, R. A. Niku, SN, 1985.A CAD system for the analysis and design of cathodic protection system. Plant Corrosion: prediction of Materials performance, Chapter 13, Institution of Corrosion Science and Technology, ELLIS HORWOOD LIMITED Publisher, Birmingham, UK.

Allahar, Kerry N. and Orazem, Mark E. 2009. On the extension of CP models to address cathodic protection under a delaminatedating. Corrosion Science 51, 962-970..

Amaya, K., Aoki, S. 2003. Effective boundary element methods in corrosion analysis. Engineering Analysis with Boundary Element 27,507-519.

Aoki, Shigeru and Amaya, Kenji. 1997. Optimization of cathodic protection system by BEM. Engineering Analysis with Boundary Element 19, 147-156.

Badawy, Waheed A., Hilal, Nadia H. El-Rabiee, Mohammed and Nady, H. 2010. Electrochemical Behavior of a Mg and some Mg alloys in aqueous solutions of different pH. Electrochimica Acta 55, 1880-1887.

Baeckmann, W. von, Schenk, W. and Prinz W., Edts, 1997. Handbook of cathodic corrosion protection. Third Edition, Gulf Publishing Company, Houston, Texas.

Baynham, J. M. E., Adey, R.A. 2008. Simulating the Transient Response of ICCP control system. Modeling of Cathodic Protection system. Modeling of Cathodic Protection Systems: R. A. Adey, Edt. WIT press, Southampton, UK. pp. 45-60.

BEASY software user guide, 2009. computational mechanics BEASY Version 10. Southampton, UK.

Brichau, F., Deconinck, J and Driesense, T. 1996. Modeling of Underground Cathodic protection Interference. Corrosion Engineering, volume.52, No.6, 480-488.

Brichau, F Deconinck, J. 1994. A Numerical Model For Cathodic Protection of Buried Pipes. Corrosion Engineering, volume.50, No.1, 39-49.

Chen, X., Li, X.G. , Du, C.W. and Cheng, Y.F. 2009. Effect of cathodic protection on corrosion of pipeline steel under disbanded coating. Corrosion Science 51, 2242-2245.

Chuang, J. M., Zamani, N.G. and Hsiung, C.C. 1987. Some computational aspects of BEM Simulation of Cathodic Protection Systems, Appl. Math. Modeling, Vol. 11, 371-379.

Cicognani, P., Gasparoni, F., Mazza, B. and Pastore, T. 1990. Application of the boundary element method to offshore Cathodic protection modeling. The electrochemical society, vol. 137, issue.6, 1689-1695.

Colominas, I., Navarrina, F. and Casteleiro, M. 1999. A boundary element formulation for the substation grounding design. Advance in Engineering Software 30, 693-700.

De Lacerda, Luiz Alkimin, De Silva, Joes Maurilio and Lazaaris, Joes. 2008. Dual Boundary element formulation for half-space cathodic protection analysis. Engineering analyses with boundary element 32, 32-40.

Degerstedt, Ross M. ,Kennelley, Kevin J., Orazem, Mark E. and Esteban, Matthew. 1996. Computer modeling aids traditional cathodic protection design methods for coated pipelines. Material Performance, Vol. 35, 16-20.

DeGiorgi, VG, Luca, KE, Thomas II, ED and Shimko, MJ. 1992. Boundary element evaluation of ICCP systems under simulated service conditions. In: Brebbia CA, Ingber MS, editors. Proceedings of BETECH92, the 7th international conference on boundary element technology; p. 405–22.

DeGiorgi, V. G., Hamilton, C.P. 1995. Coating intergrity effects on impressed current cathodic protection system parameters. Boundary Elements XVII: C. A. BREBBIA & H. POWER, Edts. Computational Mechanics Publications: Southampton, pp. 395-403.

DeGiorgi,V. G., Thomas, E.D. and Lucas, K. E. 1998. Scale effects and verification of modeling of ship cathodic protection systems. Engineering analyses with boundary element 22, 41-49**.**

DeGiorgi, V. G., Wimmer, S.A. 2005. Geometric details and modeling accuracy requirements for shipboard impress current cathodic protection system modeling. Engineering analyses with boundary element 29, 15-28.

DeGiorgi, V. G. 2002. Evaluation of Perfect Paint assumptions in modeling of cathodic protection systems. Engineering analyses with boundary element 26, 435-445.

DeGiorgi, V. G. 1997. Influence of seawater composition on corrosion prevention system parameters. Boundary element technology XII, Southampton, Computational Mechanics Publication p. 475-583.

Ditchfield, R. W., Mcgrath, J.N., Tiche-Ford, D.J. 1995. Theoretical Validation of the physical scale modeling of electrical potential characteristics of marine impressed current cathodic protection. Journal of Applied Electrochemistry 25: 54-60.

Gartland, Per. Olav, Bjoernaas, Frode and Osvoll, Harald. 1999. Computer modeling of offshore CP systems for 15 years: what have we learned? Corrosion/99 (San Antonio, TX: NACE).

Genesca, J., Betancourt, L. and Rodriguez., C. 1996 .Electrochemical Behavior of a Magnesium Galvanic Anode Under ASTM Test Method G97-89 Conditions. Corrosion Science, Vol. 52, No. 7, 0010-9312.

Humble, H. 1948. Cathodic protection of steel in seawater with magnesium anodes, *Corrosion* 4, pp. 358–370.

Jia, J. X. Song, G., Atrens, A., St John, D., Baynham, J. and Chandler, G. 2004. Evaluation of the BEASY Program using linear and piecewise linear approaches for the boundary conditions. Materials and corrosion 2004, 55, No.11, 845-852.

Jones, Denny A. 1996. Principles and Prevention of Corrosion. Second Edition, Prentice-Hall Inc., Upper Saddle River, NJ.

Kasatkin, V. E., Gelman, A. V., Zarepove, A. I., Kasatkina, I. V. and Dorofeeva, V.N. 2003 .Computer Simulation of Cathodic Protection System for Branched of Pipelines. Protection of Metals, Vol.39, 300-305.

Lee, S. H., Townley, D.W., Eshun, K.O. 1993. A Boundary Element Model of Cathodic Well Casing Protection. Journal of Computational Physics 107, 338-347.

Martinez, S. and Stern, I., 2000. A mathematical model for the internal cathodic protection of cylindrical Structures by wire anodes. Journal of applied Electrochemistry 30: 1053-1060.

Metwally, I. A. Al-Mandhari, H.M, Gastli, A. and Nadir, Z. 2007. Factors effecting interface. Engineering analyses with boundary element 31, 485-493.

Metwally, I. A. Al-Mandhari, H.M, Gastli, A. and Nadir, Z. 2008. Stray currents of ESP well casings. Engineering analyses with boundary element 32, 32-40.

Miltiadou, P. and Wrobel, L.C. 2002. Optimization of cathodic protection systems using boundary elements and Genetic Algorithms. Corrosion, Vol. 58, No. 11, 912-921.

Miltiadous, Panayiotis and Wrobel, Luiz C. 2004. "Identification of polarization Parameters of Cathodic protection system using Genetic algorithms". Engineering analyses with boundary element 28, 267-277.

Montoya, R., Rendon, O. and Genesca, J. 2005 .Mathematical simulation of a cathodic protection systems by finite element method. Materials and corrosion 2005, 56, No.6, 404-411.

NACE Standard (RP0196-2004). "Galvanic Anode Cathodic protection of Internal Submerged surface of Steel Water Storage tank" (Houston, Texas: NACE).

Orazem, M. E. Esteban, J.M., Kennelley, K.J. and Degerstedt, R.M. 1997. Mathematical Models for Cathodic protection of an underground pipeline with coating holidays. Corrosion Science, Vol. 53, No. 4, 264-272.

Osvoll, Harald, Sjaastad, Are and Duesso, Francis. 2004. Evaluation of impressed current system on FPSO'S by use of CP computer modeling. Corrosion/2004, Paper no. 4103 (New Orleans, La: NACE).

Osvoll, Harald, Gartland, pre Olav and Thomason, William H. 1995. Computer modeling of cathodic protection on Risers/Tendons. Material Performance, Vol. 34, 35-41.

Perrault, G. G. 1974 .The potential-pH Diagram of the Magnesium-Water system. Electroanalytical chemistry and Interfacial Electrochemistry, 51, 107-119.

Pinto, R., Ferreira, M.G.S., Carmezim, Montemor, M.F., 2010. Passive behavior of magnesium alloys (Mg-Zr) containing rare-earth elements in alkaline media. Electrochimica Acta, Vol. 55, 2482-2489.

Purcar, M., Bossche, B. Van den, Bortels, L., Deconinck J. and Wesselius, P. 2003. Numerical 3-D Simulation of a cathodic protection System for a Buried Pipe segment Surrounded by a Load Relieving U-Shaped Vault. Corrosion- Vol. 59, N11, 1019-1028.

Qiu, Chenchen, Orazem, Mark E. 2004. A Weighted nonlinear regression-based inverse model for interpretation of pipeline survey data. Electrochemical Acta 49, 3965-3975.

Rabiot, D., Dalard, F., Rameau, J.-J., Caire, J.-P. and Boyer, S. 1999. Study of Sacrificial anode cathodic protection of buried tanks: Numerical Modeling. Journal of applied Electrochemistry 29: 541-550.

Ramanan, V. S., Muthukumar, M., Gnanasekaran, S., Reddy, M.J. Venkataramana and Emmanuel, B. 1999. Green's function for the Laplace equation in a 3-layer medium, boundary element integrals and their application to cathodic protection. Engineering Analysis with Boundary Element 23, 777-786.

Rannou, C., Coulomb, J.L. 2006. Optimization of the cathodic protection system of military Ships with respect to the double constraint: cathodic protection and electromagnetic silencing. Presented in MARELEC Conference 2006, Amsterdam, Paper No. 193303.

Riemer, Douglas P. and Orazem, Mark E. 2005. A mathematical model for the cathodic protection of tank bottoms. Corrosion Science 47, 849-868.

Roche, Marcel and Vittonato, Jean. 2008. Cathodic protection modeling of Buoy chain Connector by 3D software simulation: Influence of holes size and coating. NACE Corrosion conference, 2008. Paper no. 8274.

Santana-Diaz, Ernesto and Adey, Rebert. 2006. "Validation of Cathodic protection design using computer simulation". The Journal of Corrosion Science and corrosion, V.6 , ISSN 1466-8858.

Santana Diaz, E., Adey, R. 2005 A. Optimising the location of anodes in cathodic protection systems to smooth potential distribution. Advance in Engineering Software 36, 591-598.

Santana-Diaz, E., Adey, R. 2005 B .Predicting the coating condition on ships using ICCP system data. International Journal for Numerical Methods in Engineering, vol. 62, 727-746.

Santiago, J. A. F., Telles, J.C.F. 1997. On boundary elements for simulation of Cathodic protection systems with Dynamic Polarization curve. International Journal for Numerical Methods In Engineering, vol. 40, 2611-2627.

Satiago, J. A. F. and Telles, J.C.F. 1999. A solution technique for cathodic protection with dynamic boundary conditions by boundary element method. Advance in Engineering Software 30, 663-671.

Strommen, R., Keim, W., Finnegan, J. and Mehdizadh, P. 1987. Advanced in offshore cathodic protection modeling using the boundary element method. Material Performance, Vol. 26, No. 2 23-28.

Sun, W. and Liu, K. M. 2000 A. Numerical Solution of Cathodic Protection System with Nonlinear Polarization Curve. The Journal Electrochemical Society 147 (10) 3687-3690.

Sun, W., Yuan, Guangwei and Ren, Y. 2000 B. Iterative algorithms for impressed cathodic protection system. International Journal for Numerical Methods in Engineering, vol. 49, 751-768.

Sun, W. 1996. "Optimal control of Impress cathodic protection systems in ship building". Appl. Math. Modeling, Vol. 20 November, 823-828.

Surkein, Michael B., La Fontains, John P. 2004. A comparison of impressed current and Galvanic Anode Cathodic Protection Design for an FPSO Hull. Corrosion/2004, Paper no. 4095 (New Orleans, La: NACE).

Wrobel, Luiz C., Miltiadous, Panayiotis. 2004. Genetic Algorithms for inverse Cathodic Protection Problems. Engineering analyses with boundary element, Vol. 28, Issue-3, 267-277.

Yan, J.-F., Pakalapati, S.N. R., Nguyen, T. V., White R.E. and Griffin R.B.**1992.** Mathematical Modeling of cathodic Protection using the boundary element method with a non-linear polarization curve. The Journal Electrochemical Society, Vol.139, No.7, 1932-1936.

Zakowski, K., Sokolski, W. 1999. Numerical method of IR elimination from measurement results of potential of underground pipelines in the zone of interaction of stray current. Corrosion Science 41, 2213-2222.

Zamani, N. G. 1988. Boundary element Simulation of the cathodic protection system in a prototype Ship. Applied Mathematics and Computation 26: 119-134.